



Measurement of the cross section for inclusive isolated-photon production in pp collisions at $\sqrt{s} = 13$ TeV using the ATLAS detector



The ATLAS Collaboration*

ARTICLE INFO

Article history:

Received 25 January 2017
 Received in revised form 31 March 2017
 Accepted 27 April 2017
 Available online 2 May 2017
 Editor: M. Doser

ABSTRACT

Inclusive isolated-photon production in pp collisions at a centre-of-mass energy of 13 TeV is studied with the ATLAS detector at the LHC using a data set with an integrated luminosity of 3.2 fb^{-1} . The cross section is measured as a function of the photon transverse energy above 125 GeV in different regions of photon pseudorapidity. Next-to-leading-order perturbative QCD and Monte Carlo event-generator predictions are compared to the cross-section measurements and provide an adequate description of the data.

© 2017 The Author(s). Published by Elsevier B.V. This is an open access article under the CC BY license (<http://creativecommons.org/licenses/by/4.0/>). Funded by SCOAP³.

1. Introduction

The production of prompt photons in proton–proton (pp) collisions, $pp \rightarrow \gamma + X$, provides a testing ground for perturbative QCD (pQCD) with a hard colourless probe. All photons produced in pp collisions that are not secondaries from hadron decays are considered as “prompt”. Two processes contribute to prompt-photon production in $pp \rightarrow \gamma + X$: the direct process, in which the photon originates directly from the hard interaction, and the fragmentation process, in which the photon is emitted in the fragmentation of a high transverse momentum (p_T) parton [1,2]. Measurements of inclusive prompt-photon production were used recently to investigate novel approaches to the description of parton radiation [3] and the importance of resummation of threshold logarithms in QCD and of the electroweak corrections [4]. Comparisons of prompt-photon data and pQCD are usually limited by the theoretical uncertainties associated with the missing higher-order terms in the perturbative expansion. The extension of the recent next-to-next-to-leading-order (NNLO) pQCD calculations for jet production [5] to prompt-photon production¹ will allow a more stringent test of pQCD. To make such a test with small experimental and theoretical uncertainties, it is optimal to perform measurements of prompt-photon production at high photon transverse energies and at the highest possible centre-of-mass energy of the colliding particles.

Since the dominant production mechanism in pp collisions at the LHC proceeds via the $qg \rightarrow q\gamma$ process, measurements of

prompt-photon production are sensitive at leading order (LO) to the gluon density in the proton [7–16]. Although prompt photon data were initially included in the determination of the proton parton distribution functions (PDFs), their use was abandoned some years ago. Since then, theoretical developments [13,14] have shown ways to improve the description of the data in terms of pQCD, and a recent study quantified the impact of prompt-photon data from hadron colliders on the gluon density in the proton [15]. New measurements of prompt-photon production at higher centre-of-mass energies are expected to further constrain the gluon density in the proton when combined with previous data.

These measurements can also be used to tune the Monte Carlo (MC) models to improve the understanding of prompt-photon production. In addition, precise measurements of these processes aid those searches for which they are an important background, such as the search for new phenomena in final states with a photon and missing transverse momentum.

Measurements of prompt-photon production at a hadron collider require isolated photons to avoid the large contribution of photons from decays of energetic π^0 and η mesons inside jets. The production of inclusive isolated photons in pp collisions at centre-of-mass energies of $\sqrt{s} = 7$ and 8 TeV was measured by the ATLAS [17–20] and CMS [21,22] collaborations.

This paper presents measurements of isolated-photon production in pp collisions at $\sqrt{s} = 13$ TeV with the ATLAS detector at the LHC using a data set with an integrated luminosity of 3.2 fb^{-1} collected during 2015. These measurements are performed in a phase-space region overlapping with that used in the previous ATLAS measurement at $\sqrt{s} = 8$ TeV [20]. Cross sections as functions

* E-mail address: atlas.publications@cern.ch.

¹ After completion of the work presented here, first NNLO calculations for prompt-photon production have been completed [6].

of the photon transverse energy² (E_T^γ) are measured in the range $E_T^\gamma > 125$ GeV for different regions of the photon pseudorapidity (η^γ). The threshold in E_T^γ is chosen so as to avoid the low- E_T^γ region where both systematic and theoretical uncertainties increase. Next-to-leading-order (NLO) pQCD and MC event-generator predictions are compared to the measurements.

2. The ATLAS detector

The ATLAS detector [23] is a multi-purpose detector with a forward-backward symmetric cylindrical geometry. It consists of an inner tracking detector surrounded by a thin superconducting solenoid, electromagnetic and hadronic calorimeters, and a muon spectrometer incorporating three large superconducting toroid magnets. The inner-detector system is immersed in a 2 T axial magnetic field and provides charged-particle tracking in the range $|\eta| < 2.5$. The high-granularity silicon pixel detector is closest to the interaction region and provides four measurements per track; the innermost layer, known as the insertable B-layer [24], was added in 2014 and provides high-resolution hits at small radius to improve the tracking performance. The pixel detector is followed by the silicon microstrip tracker, which typically provides four three-dimensional measurement points per track. These silicon detectors are complemented by the transition radiation tracker, which enables radially extended track reconstruction up to $|\eta| = 2.0$. The calorimeter system covers the range $|\eta| < 4.9$. Within the region $|\eta| < 3.2$, electromagnetic calorimetry is provided by barrel and endcap high-granularity lead/liquid-argon (LAr) electromagnetic calorimeters, with an additional thin LAr presampler covering $|\eta| < 1.8$ to correct for energy loss in material upstream of the calorimeters; for $|\eta| < 2.5$ the LAr calorimeters are divided into three layers in depth. Hadronic calorimetry is provided by a steel/scintillator-tile calorimeter, segmented into three barrel structures within $|\eta| < 1.7$, and two copper/LAr hadronic endcap calorimeters, which cover the region $1.5 < |\eta| < 3.2$. The solid angle coverage is completed out to $|\eta| = 4.9$ with forward copper/LAr and tungsten/LAr calorimeter modules, which are optimised for electromagnetic and hadronic measurements, respectively. Events are selected using a first-level trigger implemented in custom electronics, which reduces the maximum event rate of 40 MHz to a design value of 100 kHz using a subset of detector information. Software algorithms with access to the full detector information are then used in the high-level trigger to yield a recorded event rate of about 1 kHz [25].

3. Data selection

The data used in this analysis were collected with the ATLAS detector during the pp collision running period of 2015, when the LHC operated with a bunch spacing of 25 ns and a centre-of-mass energy of $\sqrt{s} = 13$ TeV. Only events taken in stable beam conditions and satisfying detector and data-quality requirements are considered. The total integrated luminosity of the collected sample amounts to $3.16 \pm 0.07 \text{ fb}^{-1}$ [26,27]. Events were recorded using a single-photon trigger, with a transverse energy threshold of 120 GeV. The trigger efficiency for isolated photons with

$E_T^\gamma > 125$ GeV and $|\eta^\gamma| < 2.37$, excluding $1.37 < |\eta^\gamma| < 1.56$, is higher than 99%.

Events are required to have a reconstructed primary vertex. Primary vertices are formed from sets of two or more reconstructed tracks, each with $p_T > 400$ MeV and $|\eta| < 2.5$, that are mutually consistent with having originated at the same three-dimensional point within the luminous region of the colliding proton beams. If multiple primary vertices are reconstructed, the one with the highest sum of the p_T^2 of the associated tracks is selected as the primary vertex.

Photon and electron candidates are reconstructed from clusters of energy deposited in the electromagnetic calorimeter. Candidates without a matching track or reconstructed conversion vertex³ in the inner detector are classified as unconverted photons [28]. Those with a matching reconstructed conversion vertex or a matching track consistent with originating from a photon conversion are classified as converted photons. Those matched to a track consistent with originating from an electron produced in the beam interaction region are classified as electrons.

The photon identification is based primarily on shower shapes in the calorimeter [28]. An initial selection is derived using the information from the hadronic calorimeter and the lateral shower shape in the second layer of the electromagnetic calorimeter, where most of the photon energy is contained. The final tight selection applies stringent criteria [28] to these variables, different for converted and unconverted photon candidates. It also places requirements on the shower shape in the finely segmented first calorimeter layer to ensure the compatibility of the measured shower profile with that originating from a single photon impacting the calorimeter. When applying the photon identification criteria to simulated events, corrections are made for small differences in the average values of the shower-shape variables between data and simulation. The efficiency of the photon identification varies in the range 92–98% for $E_T^\gamma = 125$ GeV and 86–98% for $E_T^\gamma = 1$ TeV, depending on η^γ and whether the photon candidate is classified as unconverted or converted [28,29]. For $E_T^\gamma > 125$ GeV, the uncertainty in the photon identification efficiency varies between 1% and 5%, depending on η^γ and E_T^γ .

The photon energy measurement is made using calorimeter and tracking information. A dedicated energy calibration [30] is then applied to the candidates to account for upstream energy loss and both lateral and longitudinal leakage; a multivariate regression algorithm to calibrate electron and photon energy measurements was developed and optimised on simulated events. The calibration of the layer energies in the calorimeter is based on the measurement performed with 2012 data at $\sqrt{s} = 8$ TeV [30]. The overall energy scale in data and the difference in the energy resolution's constant term⁴ between data and simulation are estimated with a sample of Z -boson decays to electrons recorded in 2012 and reprocessed using the same electron reconstruction and calibration scheme as used for the 2015 data taking and event processing. The energy scale and resolution corrections are checked using Z -boson decays to electrons recorded in the 2015 data set. Uncertainties in the measurements performed with this sample are estimated following a procedure similar to that discussed in Ref. [30]. The difference between the values measured with the 2015 data and those predicted from the reprocessed 2012 data is also taken into account in the uncertainties. The uncertainty in the photon energy scale at high E_T^γ is typically 0.5–2.0%, depending on η^γ . Events with at least one photon candidate with calibrated

² ATLAS uses a right-handed coordinate system with its origin at the nominal interaction point (IP) in the centre of the detector and the z -axis along the beam pipe. The x -axis points from the IP to the centre of the LHC ring, and the y -axis points upwards. Cylindrical coordinates (r, ϕ) are used in the transverse plane, ϕ being the azimuthal angle around the z -axis. The pseudorapidity is defined in terms of the polar angle θ as $\eta = -\ln \tan(\theta/2)$. Angular distance is measured in units of $\Delta R \equiv \sqrt{(\Delta\eta)^2 + (\Delta\phi)^2}$. The transverse energy is defined as $E_T = E \sin \theta$, where E is the energy.

³ Conversion vertex candidates are reconstructed from pairs of oppositely charged tracks in the inner detector that are likely to be electrons [28].

⁴ The relative energy resolution is parameterised as $\sigma(E)/E = a/\sqrt{E} \oplus c$, where a is the sampling term and c is the constant term.

Table 1
Kinematic requirements and number of selected events in data for each phase-space region.

Requirement on E_T^γ	Phase-space region			
	$E_T^\gamma > 125$ GeV			
Isolation requirement	$E_T^{\text{iso}} < 4.8 + 4.2 \cdot 10^{-3} \cdot E_T^\gamma$ [GeV]			
Requirement on $ \eta^\gamma $	$ \eta^\gamma < 0.6$	$0.6 < \eta^\gamma < 1.37$	$1.56 < \eta^\gamma < 1.81$	$1.81 < \eta^\gamma < 2.37$
Number of events	356 604	480 466	140 955	275 483

$E_T^\gamma > 125$ GeV and $|\eta^\gamma| < 2.37$ are selected. Candidates in the region $1.37 < |\eta^\gamma| < 1.56$, which includes the transition region between the barrel and endcap calorimeters, are not considered.

The photon candidate is required to be isolated based on the amount of transverse energy inside a cone of size $\Delta R = 0.4$ in the η - ϕ plane around the photon candidate, excluding an area of size $\Delta\eta \times \Delta\phi = 0.125 \times 0.175$ centred on the photon. The isolation transverse energy is computed from topological clusters of calorimeter cells [31] and is denoted by E_T^{iso} . The measured value of E_T^{iso} is corrected for leakage of the photon's energy into the isolation cone and the estimated contributions from the underlying event (UE) and additional inelastic pp interactions (pile-up). The latter two corrections are computed simultaneously on an event-by-event basis [18] and the combined correction is typically 2 GeV. The combined correction is computed using a method suggested in Refs. [32,33]: the k_t jet algorithm [34,35] with jet radius $R = 0.5$ is used to reconstruct all jets taking as input topological clusters of calorimeter cells; no explicit transverse momentum threshold is applied. The ambient-transverse energy density for the event (ρ), from pile-up and the underlying event, is computed using the median of the distribution of the ratio between the jet transverse energy and its area. Finally, ρ is multiplied by the area of the isolation cone to compute the correction to E_T^{iso} . In addition, for simulated events, data-driven corrections to E_T^{iso} are applied such that the peak position in the E_T^{iso} distribution coincides in data and simulation. After all these corrections, E_T^{iso} is required to be lower than $E_{T,\text{cut}}^{\text{iso}}(E_T^\gamma)$ [GeV] $\equiv 4.8 + 4.2 \cdot 10^{-3} \cdot E_T^\gamma$ [GeV] [20]. The isolation requirement significantly reduces the main background, which consists of multi-jet events where one jet typically contains a π^0 or η meson that carries most of the jet energy and is misidentified as a photon because it decays into an almost collinear photon pair.

A small fraction of the events contain more than one photon candidate satisfying the selection criteria. In such events, the highest- E_T^γ (leading) photon is considered for further study. The total number of data events selected by using the requirements discussed above amounts to 1253 508. A summary of the kinematic requirements as well as the number of selected events in data in each $|\eta^\gamma|$ region are included in Table 1. The selected sample of events is used to unfold the distribution in E_T^γ separately for each of the four regions in $|\eta^\gamma|$ indicated in Table 1; the unfolding is performed using the samples of MC events described in Section 4.1 and the results are compared to the predictions from the PYTHIA and SHERPA generators as well as to the predictions from NLO pQCD (see Section 8).

4. Monte Carlo simulations and theoretical predictions

4.1. Monte Carlo simulations

Samples of MC events were generated to study the characteristics of signal events. The MC programs PYTHIA 8.186 [36] and SHERPA 2.1.1 [37] were used to generate the simulated events. In both generators, the partonic processes were simulated using tree-level matrix elements, with the inclusion of initial- and final-state parton showers. Fragmentation into hadrons was performed

using the Lund string model [38] in the case of PYTHIA, and in SHERPA events by a modified version of the cluster model [39]. The LO NNPDF2.3 [40] PDFs were used for PYTHIA (NLO CT10 [41] for SHERPA) to parameterise the proton structure. Both samples include a simulation of the UE. The event-generator parameters were set according to the ‘‘A14’’ tune for PYTHIA [42] and the ‘‘CT10’’ tune for SHERPA. All the samples of generated events were passed through the GEANT4-based [43] ATLAS detector- and trigger-simulation programs [44]. They were reconstructed and analysed by the same program chain as the data. Pile-up from additional pp collisions in the same and neighbouring bunch crossings was simulated by overlaying each MC event with a variable number of simulated inelastic pp collisions generated using PYTHIA8 with the A2 tune [45]. The MC events were weighted to reproduce the distribution of the average number of interactions per bunch crossing (μ) observed in the data, referred to as ‘‘pile-up reweighting’’; in this procedure, the μ value in the data is divided by a factor of 1.16 ± 0.07 , a rescaling which improves the agreement between the data and simulation for the observed number of primary vertices and recovers the fraction of visible cross-section of inelastic pp collisions as measured in the data [46].

The PYTHIA simulation of the signal includes LO photon-plus-jet events from both direct processes (the hard subprocesses $qg \rightarrow q\gamma$ and $q\bar{q} \rightarrow g\gamma$, called the ‘‘hard’’ component) and photon bremsstrahlung in QCD dijet events (called the ‘‘bremsstrahlung’’ component). The SHERPA samples were generated with LO matrix elements for photon-plus-jet final states with up to three additional partons ($2 \rightarrow n$ processes with n from 2 to 5); the matrix elements were merged with the SHERPA parton shower [47] using the ME+PS@LO prescription. While the bremsstrahlung component was modelled in PYTHIA by final-state QED radiation arising from calculations of all $2 \rightarrow 2$ QCD processes, it was accounted for in SHERPA through the matrix elements of $2 \rightarrow n$ processes with $n \geq 3$; in the generation of the SHERPA samples, a requirement on the photon isolation at the matrix-element level was imposed using the criterion defined in Ref. [48].⁵

The predictions of the MC generators at particle level are defined using those particles with a lifetime τ longer than 10 ps; these particles are referred to as ‘‘stable’’. The particles associated with the overlaid pp collisions (pile-up) are not considered. The particle-level isolation requirement on the photon was built summing the transverse energy of all stable particles, except for muons and neutrinos, in a cone of size $\Delta R = 0.4$ around the photon direction after the contribution from the UE was subtracted; the same subtraction procedure used on data was applied at the particle level. Therefore, the cross sections quoted from MC simulations refer to photons that are isolated by requiring $E_T^{\text{iso}}(\text{particle}) < E_{T,\text{cut}}^{\text{iso}}(E_T^\gamma)$.

⁵ This criterion, commonly called Frixiore's criterion, requires the total transverse energy inside a cone of size \mathcal{V} around the generated final-state photon, excluding the photon itself, to be below a certain threshold, $E_T^{\text{max}}(\mathcal{V}) = \epsilon E_T^\gamma ((1 - \cos \mathcal{V}) / (1 - \cos \mathcal{R}))^n$, for all $\mathcal{V} < \mathcal{R}$. The parameters for the threshold were chosen to be $\mathcal{R} = 0.3$, $n = 2$ and $\epsilon = 0.025$.

4.2. Next-to-leading-order pQCD predictions

The NLO pQCD predictions presented in this paper are computed using the program `JETPHOX 1.3.1_2` [49,13]. This program includes a full NLO pQCD calculation of both the direct and fragmentation contributions to the cross section for the $pp \rightarrow \gamma + X$ process.

The number of massless quark flavours is set to five. The renormalisation scale μ_R (at which the strong coupling is evaluated), factorisation scale μ_F (at which the proton PDFs are evaluated) and fragmentation scale μ_f (at which the fragmentation function is evaluated) are chosen to be $\mu_R = \mu_F = \mu_f = E_T^\gamma$. The calculations are performed using the MMHT2014 [50] parameterisations of the proton PDFs and the BFG set II of parton-to-photon fragmentation functions at NLO [51]. The strong coupling constant is calculated at two loops with $\alpha_s(m_Z) = 0.120$. Predictions based on other proton PDF sets, namely CT14 [52] and NNPDF3.0 [53], are also computed. The calculations are performed using a parton-level isolation criterion which requires the total transverse energy from the partons inside a cone of size $\Delta R = 0.4$ around the photon direction to be below $E_{T,\text{cut}}^{\text{iso}}(E_T^\gamma)$.

The NLO pQCD predictions refer to the parton level while the measurements refer to the particle level. Since the data are corrected for pile-up and UE effects and the distributions are unfolded to a phase-space definition in which the requirement on E_T^{iso} at particle level is applied after subtraction of the UE, it is expected that parton-to-hadron corrections to the NLO pQCD predictions are small. This is confirmed by computing the ratio of the particle-level cross section for a PYTHIA sample with UE effects to the parton-level cross section without UE effects⁶: the ratio is consistent with unity within 1% over the measured range in E_T^γ . Therefore, no correction is applied to the NLO pQCD predictions and an uncertainty of 1% is assigned.

5. Background estimation and signal extraction

A non-negligible background contribution remains in the selected sample, even after imposing the tight identification and isolation requirements on the photon. This background originates mainly from multi-jet processes in which a jet is misidentified as a photon.

The background subtraction relies on a data-driven method based on signal-suppressed control regions. The background contamination in the selected sample is estimated using the same two-dimensional sideband technique as in the previous analyses [17,18,54,20,55] and then subtracted bin-by-bin from the observed yield. In this method, the photon is classified as:

- “isolated”, if $E_T^{\text{iso}} < E_{T,\text{cut}}^{\text{iso}}(E_T^\gamma)$;
- “non-isolated”, if $E_T^{\text{iso}} > E_{T,\text{cut}}^{\text{iso}}(E_T^\gamma) + 2 \text{ GeV}$ and $E_T^{\text{iso}} < 50 \text{ GeV}$;
- “tight”, if it satisfies the tight photon identification criteria;
- “non-tight”, if it fails at least one of four tight requirements on the shower-shape variables computed from the energy deposits in the first layer of the electromagnetic calorimeter, but satisfies the tight requirement on the total lateral shower width in the first layer and all the other tight identification criteria [28].

In the two-dimensional plane formed by E_T^{iso} and the photon identification variables, which are chosen because they are ex-

pected to be independent for the background, four regions are defined:

- *A*: the “signal” region, containing tight isolated photon candidates;
- *B*: the “non-isolated” background control region, containing tight non-isolated photon candidates;
- *C*: the “non-tight” background control region, containing isolated non-tight photon candidates;
- *D*: the background control region containing non-isolated non-tight photon candidates.

The signal yield N_A^{sig} in region *A* is estimated by using the relation

$$N_A^{\text{sig}} = N_A - R^{\text{bg}} \cdot (N_B - f_B N_A^{\text{sig}}) \cdot \frac{(N_C - f_C N_A^{\text{sig}})}{(N_D - f_D N_A^{\text{sig}})}, \quad (1)$$

where N_K , with $K = A, B, C, D$, is the number of events in region *K* and $R^{\text{bg}} = N_A^{\text{bg}} \cdot N_D^{\text{bg}} / (N_B^{\text{bg}} \cdot N_C^{\text{bg}})$ is the so-called background correlation and is taken as $R^{\text{bg}} = 1$ for the nominal results; N_K^{bg} with $K = A, B, C, D$ is the number of background events in each region. Equation (1) takes into account the expected number of signal events in the three background control regions (N_K^{sig}) via the signal leakage fractions, $f_K = N_K^{\text{sig}} / N_A^{\text{sig}}$ with $K = B, C, D$, which are estimated using the MC simulations of the signal. A systematic uncertainty is assigned to the modelling of the signal leakage fractions (see Section 7.1). The only assumption underlying Eq. (1) is that the isolation and identification variables are independent for background events, thus $R^{\text{bg}} = 1$. This assumption is verified both in simulated background samples and in data in a background-dominated region [20]. A study of R^{bg} in background-dominated regions, accounting for signal leakage using either the PYTHIA or SHERPA simulations, shows deviations from unity which are then propagated through Equation (1) and taken as systematic uncertainties. The signal purity, defined as N_A^{sig} / N_A , is above 90% for $E_T^\gamma = 125 \text{ GeV}$ in all η^γ regions and increases as E_T^γ increases. The signal purity is similar whether PYTHIA or SHERPA is used to extract the signal leakage fractions and the difference is taken as a systematic uncertainty.

There is an additional background from electrons misidentified as photons, mainly produced in Drell-Yan $Z^{(*)}/\gamma^* \rightarrow e^+e^-$ and $W^{(*)} \rightarrow e\nu$ processes. Such misidentified electrons are largely suppressed by the photon selection. The remaining electron background is estimated using MC techniques and found to be negligible in the phase-space region of the analysis presented here.

6. Unfolding

The isolated-photon cross section is measured as a function of E_T^γ in different regions of $|\eta^\gamma|$. The phase-space regions are listed in Table 1. The data distributions, after background subtraction, are unfolded to the particle level using bin-by-bin correction factors determined using the MC samples. These correction factors take into account the efficiency of the selection criteria and the purity and efficiency of the photon reconstruction. The data distributions are unfolded to the particle level via the formula

$$\frac{d\sigma}{dE_T^\gamma}(i) = \frac{N_A^{\text{sig}}(i) C^{\text{MC}}(i)}{\mathcal{L} \Delta E_T^\gamma(i)}, \quad (2)$$

where $(d\sigma/dE_T^\gamma)(i)$ is the cross section as a function of the observable E_T^γ in bin *i*, $N_A^{\text{sig}}(i)$ is the number of background-subtracted data events in bin *i*, $C^{\text{MC}}(i)$ is the correction factor in bin *i*, \mathcal{L} is

⁶ The effects of hadronisation and UE are also studied separately; the effects of including the UE do not cancel those of hadronisation and are dominant.

the integrated luminosity and $\Delta E_T^\gamma(i)$ is the width of bin i . The correction factors are computed using the MC samples of events as $C^{\text{MC}}(i) = N_{\text{part}}^{\text{MC}}(i)/N_{\text{reco}}^{\text{MC}}(i)$, where $N_{\text{part}}^{\text{MC}}(i)$ is the number of events which satisfy the kinematic constraints of the phase-space region at the particle level, and $N_{\text{reco}}^{\text{MC}}(i)$ is the number of events which meet all the selection criteria at the reconstruction level.

The nominal cross sections are measured using the correction factors from PYTHIA and the deviations from these results when using SHERPA to unfold the data are taken to represent systematic uncertainties in how the parton-shower and hadronisation models affect the corrections. The correction factors increase as E_T^γ increases and vary between 1.04 and 1.24 depending on E_T^γ and η^γ . The results of the bin-by-bin unfolding procedure are checked with a Bayesian unfolding method [56], giving consistent results.

7. Experimental and theoretical uncertainties

7.1. Experimental uncertainties

The primary sources of systematic uncertainty that affect the measurements are investigated. These sources include photon identification, photon energy scale and resolution, background subtraction, modelling of the final state, pile-up, MC sample statistics, trigger and luminosity.

- **Photon identification efficiency.** The uncertainty in the photon identification efficiency is estimated from the effect of differences between shower-shape variable distributions in data and simulation. From the studies presented in Ref. [28], this procedure is found to provide a conservative estimate of the uncertainties.⁷ The resulting uncertainty in the measured cross sections increases from 1–2% at $E_T^\gamma = 125$ GeV to 2–6% at $E_T^\gamma \sim 1$ TeV.
- **Photon energy scale and resolution.** A detailed assessment of the uncertainties in the photon energy scale and resolution is made using the same method developed with 8 TeV data [30]. The sources of uncertainty include: the uncertainty in the overall energy scale adjustment using $Z \rightarrow e^+e^-$; the uncertainty in the non-linearity of the energy measurement at the cell level; the uncertainty in the relative calibration of the different calorimeter layers; the uncertainty in the amount of material in front of the calorimeter; the uncertainty in the modelling of the reconstruction of photon conversions; the uncertainty in the modelling of the lateral shower shape; the uncertainty in the modelling of the sampling term; the uncertainty in the modelling of the sampling term; the uncertainty in the measurement of the constant term in Z -boson decays. Additional systematic uncertainties are included to take into account the differences between the 2012 and 2015 configurations. These uncertainties are modelled using independent components to account for their η dependence. All the components are propagated through the analysis separately to maintain the full information about the correlations. The systematic uncertainties in the measured cross sections due to the effects mentioned above are estimated by varying by $\pm 1\sigma$ each individual source of uncertainty separately in the MC simulations and then added in quadrature. The resulting uncertainty increases from about 2% at $E_T^\gamma = 125$ GeV to about 5% at $E_T^\gamma \sim 1$ TeV except in the $1.56 < |\eta^\gamma| < 1.81$

region, where it increases from about 7% at $E_T^\gamma = 125$ GeV to about 18% at $E_T^\gamma \sim 1$ TeV.

- **Definition of the background control regions.** The estimation of the background contamination in the signal region is affected by the choice of background control regions. The control regions B and D are defined by the lower and upper limits on E_T^{iso} and the choice of inverted photon identification variables used in the selection of non-tight photons. To study the dependence on the specific choices, these definitions are varied over a wide range. The lower limit on E_T^{iso} in regions B and D is varied by ± 1 GeV, which is larger than any difference between data and simulations and still provides a sufficient sample to perform the data-driven subtraction. The upper limit on E_T^{iso} in regions B and D is removed. The resulting uncertainty in the measured cross sections is negligible. Likewise, the choice of inverted photon identification variables is varied. The analysis is repeated using different sets of variables: tighter (looser) identification criteria are defined by applying tight requirements to an extended (restricted) set of shower-shape variables in the first calorimeter layer. The resulting uncertainty in the measured cross sections is typically smaller than 2%.
- **Photon identification and isolation correlation in the background.** The photon isolation and identification variables used to define the plane in the two-dimensional sideband method to subtract the background are assumed to be independent for background events ($R^{\text{bg}} = 1$ in Eq. (1)). Any correlation between these variables affects the estimation of the purity of the signal and leads to systematic uncertainties in the background-subtraction procedure. A range in R^{bg} is set to cover the deviations from unity observed for the estimations based on subtracting the signal leakage with either PYTHIA or SHERPA MC samples. The resulting range in R^{bg} , which is taken as the uncertainty, is $0.8 < R^{\text{bg}} < 1.2$ for $0.6 < |\eta^\gamma| < 1.37$ and $1.81 < |\eta^\gamma| < 2.37$; for the region $|\eta^\gamma| < 0.6$ ($1.56 < |\eta^\gamma| < 1.81$), the range is $0.8 < R^{\text{bg}} < 1.2$ ($0.75 < R^{\text{bg}} < 1.25$) at low E_T^γ and increases to $0.65 < R^{\text{bg}} < 1.35$ ($0.6 < R^{\text{bg}} < 1.4$) at high E_T^γ . The resulting uncertainty in the measured cross sections is typically smaller than 2%.
- **Parton-shower and hadronisation model dependence.** The effects due to the parton-shower and hadronisation models in the signal purity and correction factors are studied separately; the effects are estimated as the differences observed between the nominal results and those obtained using SHERPA MC samples either for the determination of the signal leakage fractions or the unfolding correction factors. The resulting uncertainties in the measured cross sections are typically smaller than 2%.
- **Photon isolation modelling.** The differences between the nominal results and those obtained without applying the data-driven corrections to E_T^{iso} in simulated events are taken as systematic uncertainties in the measurements due to the modelling of E_T^{iso} in the MC simulation. The resulting uncertainty in the measured cross sections is smaller than 2%.
- **Signal modelling.** The MC simulation of the signal is used to estimate the signal leakage fractions in the two-dimensional sideband method for background subtraction and to compute the bin-by-bin correction factors. The PYTHIA simulation is used with the mixture of the hard and bremsstrahlung components as predicted by the generator to yield the background-subtracted data distributions and to compute the correction factors; in the predicted mixture, the relative contribution of the bremsstrahlung component amounts to $\approx 30\%$. The uncertainty related to the simulation of the hard and bremsstrahlung components is estimated by performing the background subtraction and the calculation of the correction

⁷ The photon identification efficiencies from data-driven methods and MC simulations were compared in Ref. [28]. No significant difference is observed between the data-driven measurements and the nominal or corrected (for the small differences in the average values of the shower-shape variables between data and simulation) simulation for $E_T^\gamma > 60$ GeV.

factors using a mixture with either two or zero times the amount of the bremsstrahlung component. The resulting uncertainty in the measured cross sections is typically smaller than 1%.

- **Pile-up.** The uncertainty is estimated by changing the nominal rescaling factor of 1.16 from 1.09 to 1.23 and re-evaluating the reweighting factors. The resulting uncertainty in the measured cross sections is typically smaller than 0.5%.

The total systematic uncertainty is computed by adding in quadrature the uncertainties from the sources listed above and the statistical uncertainty of the MC samples as well as the uncertainty in the trigger efficiency. The uncertainty in the integrated luminosity is 2.1% [27]. This uncertainty is fully correlated in all bins of all the measured cross sections and is shown separately. The total systematic uncertainty is smaller than 5% for $|\eta^\gamma| < 1.37$. For $1.56 < |\eta^\gamma| < 1.81$ ($1.81 < |\eta^\gamma| < 2.37$), it increases from $\approx 8\%$ (4%) at $E_T^\gamma = 125$ GeV to $\approx 19\%$ (11%) at the high end of the spectrum. For $E_T^\gamma \lesssim 600$ GeV, the systematic uncertainty dominates the total experimental uncertainty, while for higher E_T^γ values, the statistical uncertainty of the data limits the precision of the measurements.

7.2. Theoretical uncertainties

The following sources of uncertainty in the theoretical predictions are considered:

- The uncertainty in the NLO pQCD predictions due to terms beyond NLO is estimated by repeating the calculations using values of μ_R , μ_F and μ_f scaled by the factors 0.5 and 2. The three scales are either varied simultaneously, individually or by fixing one and varying the other two. In all cases, the condition $0.5 \leq \mu_A/\mu_B \leq 2$ is imposed, where $A, B = R, F, f$ and $A \neq B$. The final uncertainty is taken as the largest deviation from the nominal value among the 14 possible variations.
- The uncertainty in the NLO pQCD predictions due to imperfect knowledge of the proton PDFs is estimated by repeating the calculations using the 50 sets from the MMHT2014 error analysis [50] and applying the Hessian method [57,58] for evaluation of the PDF uncertainties.
- The uncertainty in the NLO pQCD predictions due to that in the value of $\alpha_s(m_Z)$ is estimated by repeating the calculations using two additional sets of proton PDFs from the MMHT2014 analysis, for which different values of $\alpha_s(m_Z)$ were assumed in the fits, namely $\alpha_s(m_Z) = 0.118$ and 0.122 ; in this way, the correlation between α_s and the PDFs is preserved.
- An uncertainty of 1% is assigned due to the non-perturbative effects of hadronisation and UE (see Section 4.2).

The dominant theoretical uncertainty is that arising from the terms beyond NLO and amounts to 10–15% for all η^γ regions. The uncertainty arising from those in the PDFs increases from 1% at $E_T^\gamma = 125$ GeV to 3–4% at high E_T^γ . The uncertainty arising from the value of $\alpha_s(m_Z)$ is below 2%. The total theoretical uncertainty is obtained by adding in quadrature the individual uncertainties listed above and amounts to 10–15%.

8. Results

Fig. 1 shows the isolated-photon cross section as a function of E_T^γ in four different regions of η^γ . The measured cross sections decrease by approximately five orders of magnitude in the measured range. Values of E_T^γ up to 1.5 TeV are accessed. The cross-section distributions measured in the four different regions of η^γ have similar shapes.

The predictions of the PYTHIA and SHERPA MC models are compared to the measurements in Fig. 1. These predictions are normalised to the measured integrated cross section in each η^γ region. The difference in normalisation between data and PYTHIA (SHERPA) is $\sim +10\%$ ($+30\%$) and attributed to the fact that these generators are based on tree-level matrix elements, which are affected by a large normalisation uncertainty due to missing higher-order terms. The predictions of both PYTHIA and SHERPA give a good description of the shape of the measured cross-section distributions for $E_T^\gamma \lesssim 500$ GeV in the range $|\eta^\gamma| < 1.37$ and in the whole measured E_T^γ range for $1.56 < |\eta^\gamma| < 2.37$.

Fig. 2 shows the measured isolated-photon cross sections as functions of E_T^γ in four different regions of η^γ compared with the predictions of the NLO pQCD calculations of JETPHOX based on the MMHT2014 proton PDF set. The ratios of the theoretical predictions based on different PDF sets to the measured cross sections are shown in Fig. 3. The predictions based on MMHT2014, CT14 and NNPDF3.0 are very similar, the differences being much smaller than the theoretical scale uncertainties. For most of the points, the theoretical uncertainties are larger than those of experimental origin. Differences are observed between data and the predictions of up to 10–15% depending on E_T^γ and $|\eta^\gamma|$; since the theoretical uncertainties are 10–15% and cover those differences, it is concluded that the NLO pQCD predictions provide an adequate description of the measurements.

The measured cross sections are larger than those at $\sqrt{s} = 8$ TeV [20] by approximately a factor of two at low E_T^γ ($E_T^\gamma \sim 125$ GeV) and by approximately an order of magnitude at the high end of the spectrum in each region of $|\eta^\gamma|$. Such increases in the measured cross section are expected from the increase in the centre-of-mass energy. The experimental uncertainties of the measurements at $\sqrt{s} = 8$ and 13 TeV are comparable. For both centre-of-mass energies the NLO theoretical uncertainties are of similar size and comparable to the differences between the predictions and the data; since, in addition, the experimental uncertainties are smaller than those differences, the inclusion of NNLO pQCD corrections might improve the description of the two sets of measurements.

The measured fiducial cross section for inclusive isolated-photon production in the phase-space region given by $E_T^\gamma > 125$ GeV and $|\eta^\gamma| < 2.37$ (excluding the region of $1.37 < |\eta^\gamma| < 1.56$) and isolation $E_T^{\text{iso}} < E_{T,\text{cut}}^{\text{iso}}(E_T^\gamma)$ is

$$\sigma_{\text{meas}} = 399 \pm 13 \text{ (exp.)} \pm 8 \text{ (lumi.) pb},$$

where “exp.” denotes the sum in quadrature of the statistical and systematic uncertainties and “lumi.” denotes the uncertainty due to that in the integrated luminosity, details of which are listed in Table 2.

The fiducial cross section predicted at NLO in pQCD by JETPHOX using the MMHT2014 PDFs is

$$\sigma_{\text{NLO}} = 352_{-29}^{+36} \text{ (scale)} \pm 3 \text{ (PDF)} \pm 6 \text{ } (\alpha_s) \\ \pm 4 \text{ (non-perturb.) pb},$$

which is 12% lower than the measurement, but consistent within the experimental and theoretical uncertainties.

9. Summary

A measurement of the cross section for inclusive isolated-photon production in pp collisions at $\sqrt{s} = 13$ TeV with the ATLAS detector at the LHC is presented using a data set with an integrated luminosity of 3.2 fb^{-1} . Cross sections as functions of E_T^γ are measured in four different regions of η^γ for photons with

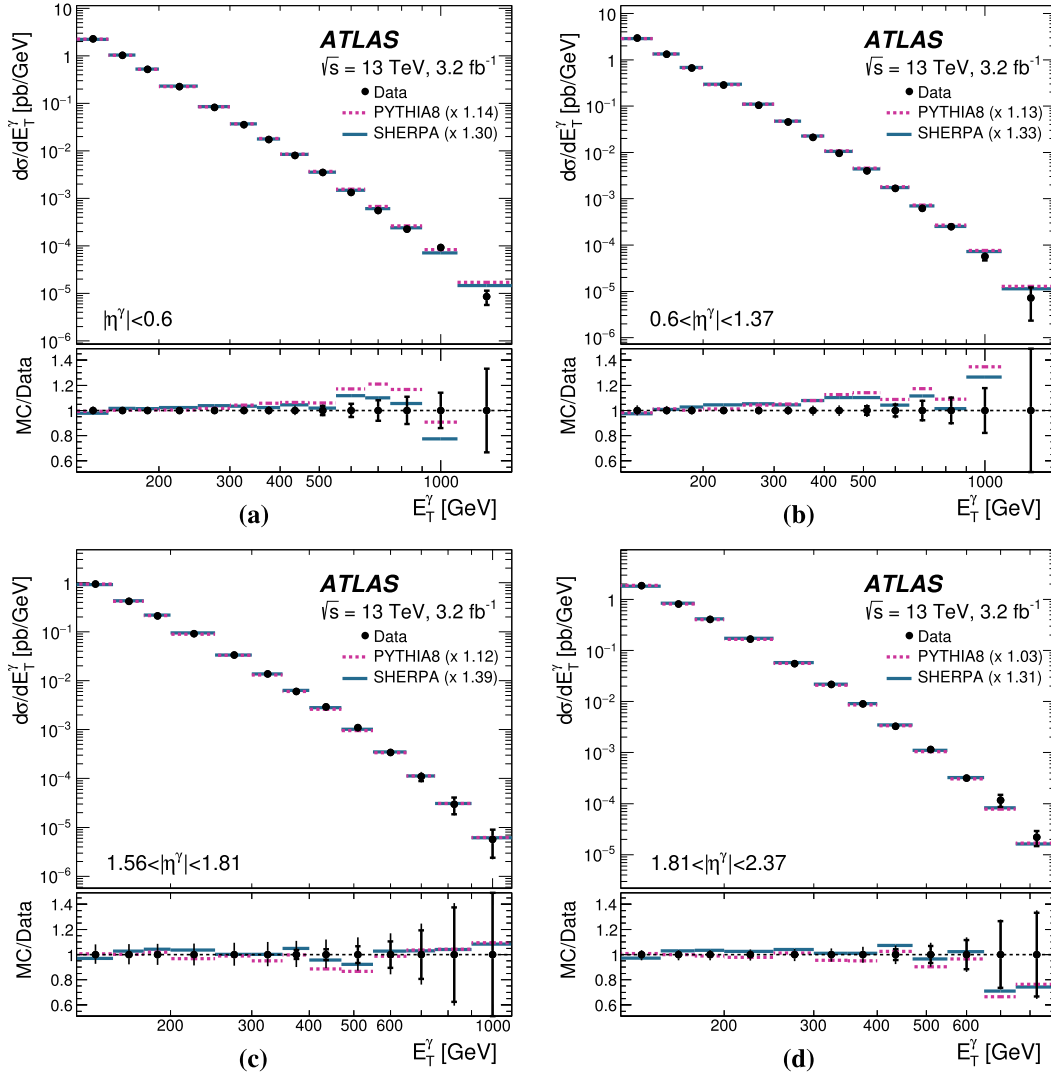


Fig. 1. Measured cross sections for isolated-photon production (dots) as functions of E_T^γ in (a) $|\eta^\gamma| < 0.6$, (b) $0.6 < |\eta^\gamma| < 1.37$, (c) $1.56 < |\eta^\gamma| < 1.81$ and (d) $1.81 < |\eta^\gamma| < 2.37$. The predictions from PYTHIA (dashed lines) and SHERPA (solid lines) are also shown; these predictions are normalised to the measured integrated cross section in each region of $|\eta^\gamma|$ using the values indicated in parentheses. The bottom part of each figure shows the ratio of the MC predictions to the measured cross section. The inner (outer) error bars represent the statistical uncertainties (the statistical and systematic uncertainties, excluding that on the luminosity, added in quadrature). For most of the points, the inner error bars are smaller than the marker size and, thus, not visible.

Table 2

Uncertainties (in pb) in the fiducial cross section: photon identification (“ γ ID”), photon energy scale and resolution (“ γ ES+ER”), lower limit in E_T^{iso} in regions B and D (“ E_T^{iso} Gap”), removal of upper limit in E_T^{iso} in regions B and D (“ E_T^{iso} upp. lim.”), variation of the inverted photon identification variables (“ γ invert. var.”), correlation between γ ID and isolation in the background (“ R^{bg} ”), signal leakage fractions of SHERPA (“Leak. SHERPA”), unfolding with SHERPA (“Unf. SHERPA”), modelling of E_T^{iso} in MC simulation (“ E_T^{iso} MC”), mixture of hard and bremsstrahlung components in MC samples (“Hard and Brem”), pile-up (“Pile-up”), statistical uncertainty in MC samples (“MC stat.”), trigger (“Trigger”), statistical uncertainty in data (“Data stat.”) and luminosity (“Luminosity”).

Uncertainties [pb]					
γ ID	(−5.2, +5.4)	γ ES+ER	(−7.9, +8.4)	E_T^{iso} Gap	±0.3
E_T^{iso} upp. lim.	+0.6	γ invert. var.	(−4.1, +3.5)	R^{bg}	(−6.2, +6.1)
Leak. SHERPA	±4.1	Unf. SHERPA	±2.9	E_T^{iso} MC	−2.8
Hard and Brem	(−1.0, +1.9)	Pile-up	(−1.1, +1.3)	MC stat.	±0.4
Trigger	±1.1	Data stat.	±0.4	Luminosity	±8.4

$E_T^\gamma > 125$ GeV and $|\eta^\gamma| < 2.37$, excluding the region $1.37 < |\eta^\gamma| < 1.56$. Selection of isolated photons is ensured by requiring that the transverse energy in a cone of size $\Delta R = 0.4$ around the photon is smaller than $4.8 + 4.2 \cdot 10^{-3} \cdot E_T^\gamma$ [GeV]. Values of E_T^γ up to 1.5 TeV are measured. The fiducial cross section is measured to be $\sigma_{\text{meas}} = 399 \pm 13$ (exp.) ± 8 (lumi.) pb.

The experimental systematic uncertainties are evaluated such that the correlations with previous ATLAS measurements of prompt-photon production can be used in the fits of the proton parton distribution functions. A combined fit at NNLO pQCD of the measurements in pp collisions at centre-of-mass energies of 8 and 13 TeV which takes into account the correlated systematic uncer-

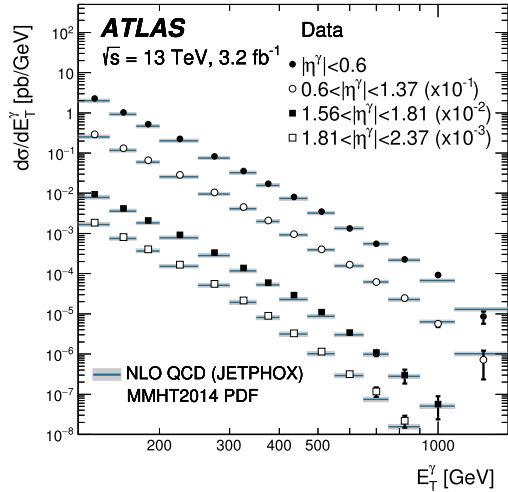


Fig. 2. Measured cross sections for isolated-photon production as functions of E_T^γ in $|\eta^\gamma| < 0.6$ (black dots), $0.6 < |\eta^\gamma| < 1.37$ (open circles), $1.56 < |\eta^\gamma| < 1.81$ (black squares) and $1.81 < |\eta^\gamma| < 2.37$ (open squares). The NLO pQCD predictions from JETPHOX based on the MMHT2014 PDFs (solid lines) are also shown. The measurements and the predictions are normalised by the factors shown in parentheses to aid visibility. The error bars represent the statistical and systematic uncertainties added in quadrature. The shaded bands display the theoretical uncertainty.

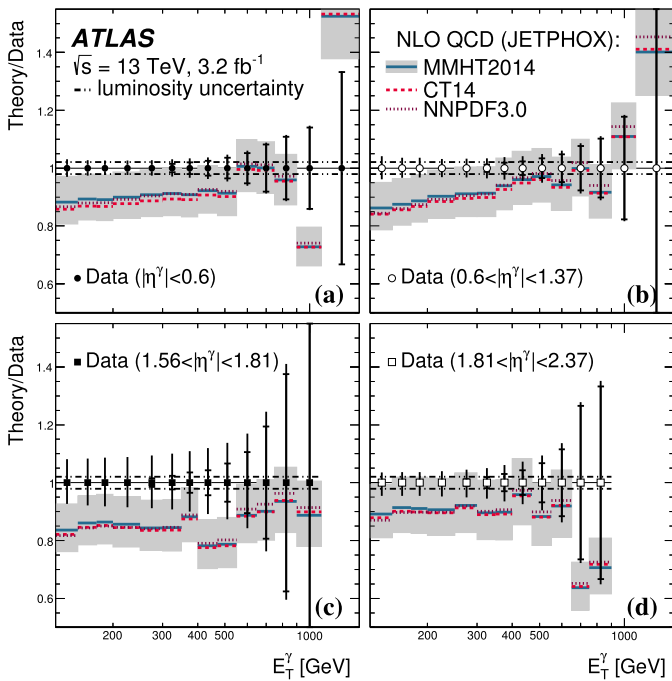


Fig. 3. Ratio of the NLO pQCD predictions from JETPHOX based on the MMHT2014 PDFs to the measured cross sections for isolated-photon production (solid lines) as a function of E_T^γ in (a) $|\eta^\gamma| < 0.6$, (b) $0.6 < |\eta^\gamma| < 1.37$, (c) $1.56 < |\eta^\gamma| < 1.81$ and (d) $1.81 < |\eta^\gamma| < 2.37$. The inner (outer) error bars represent the statistical uncertainties (statistical and systematic uncertainties, excluding that on the luminosity, added in quadrature), the dot-dashed lines represent the uncertainty due to the luminosity measurement and the shaded bands display the theoretical uncertainty of the calculation based on the MMHT2014 PDFs. The ratio of the NLO pQCD predictions based on the CT14 (dashed lines) or NNPDF3.0 (dotted lines) PDF sets to the data are also included.

tainties has the potential to constrain further the proton PDFs than either set of measurements alone.

The predictions of the PYTHIA and SHERPA Monte Carlo models give a good description of the shape of the measured cross-section distributions except for $E_T^\gamma \gtrsim 500$ GeV in the regions $|\eta^\gamma| < 0.6$

and $0.6 < |\eta^\gamma| < 1.37$. The next-to-leading-order pQCD predictions, using JETPHOX and based on different sets of proton PDFs, provide an adequate description of the data within the experimental and theoretical uncertainties. For most of the phase space the theoretical uncertainties are larger than those of experimental nature and dominated by the terms beyond NLO, from which it is concluded that NNLO pQCD corrections are needed to make an even more stringent test of the theory.

Acknowledgements

We thank CERN for the very successful operation of the LHC, as well as the support staff from our institutions without whom ATLAS could not be operated efficiently.

We acknowledge the support of ANPCyT, Argentina; YerPhI, Armenia; ARC, Australia; BMWFW and FWF, Austria; ANAS, Azerbaijan; SSTC, Belarus; CNPq and FAPESP, Brazil; NSERC, NRC and CFI, Canada; CERN; CONICYT, Chile; CAS, MOST and NSFC, China; COLCIENCIAS, Colombia; MSMT CR, MPO CR and VSC CR, Czech Republic; DNRF and DNSRC, Denmark; IN2P3-CNRS, CEA-DSM/IRFU, France; SNSF, Georgia; BMBF, HGF, and MPG, Germany; GSRT, Greece; RGC, Hong Kong SAR, China; ISF, I-CORE and Benoziyo Center, Israel; INFN, Italy; MEXT and JSPS, Japan; CNRST, Morocco; NWO, Netherlands; RCN, Norway; MNiSW and NCN, Poland; FCT, Portugal; MNE/IFA, Romania; MES of Russia and NRC KI, Russian Federation; JINR; MESTD, Serbia; MSSR, Slovakia; ARRS and MIZŠ, Slovenia; DST/NRF, South Africa; MINECO, Spain; SRC and Wallenberg Foundation, Sweden; SERI, SNSF and Cantons of Bern and Geneva, Switzerland; MOST, Taiwan; TAEK, Turkey; STFC, United Kingdom; DOE and NSF, United States of America. In addition, individual groups and members have received support from BCKDF, the Canada Council, CANARIE, CRC, Compute Canada, FQRNT, and the Ontario Innovation Trust, Canada; EPLANET, ERC, ERDF, FP7, Horizon 2020 and Marie Skłodowska-Curie Actions, European Union; Investissements d'Avenir Labex and Idex, ANR, Région Auvergne and Fondation Partager le Savoir, France; DFG and AvH Foundation, Germany; Herakleitos, Thales and Aristeia programmes co-financed by EU-ESF and the Greek NSRF; BSF, GIF and Minerva, Israel; BRF, Norway; CERCA Programme Generalitat de Catalunya, Generalitat Valenciana, Spain; the Royal Society and Leverhulme Trust, United Kingdom.

The crucial computing support from all WLCG partners is acknowledged gratefully, in particular from CERN, the ATLAS Tier-1 facilities at TRIUMF (Canada), NDGF (Denmark, Norway, Sweden), CC-IN2P3 (France), KIT/GridKA (Germany), INFN-CNAF (Italy), NL-T1 (Netherlands), PIC (Spain), ASGC (Taiwan), RAL (UK) and BNL (USA), the Tier-2 facilities worldwide and large non-WLCG resource providers. Major contributors of computing resources are listed in Ref. [59].

References

- [1] T. Pietrycki, A. Szczurek, Photon-jet correlations in pp and pp collisions, *Phys. Rev. D* 76 (2007) 034003, arXiv:0704.2158 [hep-ph].
- [2] Z. Belghobsi, et al., Photon-jet correlations and constraints on fragmentation functions, *Phys. Rev. D* 79 (2009) 114024, arXiv:0903.4834 [hep-ph].
- [3] A.V. Lipatov, M.A. Malyshev, Reconsideration of the inclusive prompt photon production at the LHC with k_T -factorization, *Phys. Rev. D* 94 (2016) 034020, arXiv:1606.02696 [hep-ph].
- [4] M.D. Schwartz, Precision direct photon spectra at high energy and comparison to the 8 TeV ATLAS data, *J. High Energy Phys.* 1609 (2016) 005, arXiv:1606.02313 [hep-ph].
- [5] J. Currie, E.W.N. Glover, J. Pires, NNLO QCD predictions for single jet inclusive production at the LHC, *Phys. Rev. Lett.* 118 (2017) 072002, arXiv:1611.01460 [hep-ph].
- [6] J.M. Campbell, R.K. Ellis, C. Williams, Direct photon production at next-to-next-to-leading order, arXiv:1612.04333 [hep-ph], 2016.

- [7] D.W. Duke, J.F. Owens, Q^2 dependent parametrizations of parton distribution functions, *Phys. Rev. D* 30 (1984) 49.
- [8] J.F. Owens, Large momentum transfer production of direct photons, jets, and particles, *Rev. Mod. Phys.* 59 (1987) 465.
- [9] P. Aurenche, R. Baier, M. Fontannaz, D. Schiff, Prompt photon production at large p_T scheme invariant QCD predictions and comparison with experiment, *Nucl. Phys. B* 297 (1988) 661.
- [10] A.D. Martin, R.G. Roberts, W.J. Stirling, Structure function analysis and ψ , Jet, W, Z production: pinning down the gluon, *Phys. Rev. D* 37 (1988) 1161.
- [11] P. Aurenche, R. Baier, M. Fontannaz, J.F. Owens, M. Werlen, The gluon contents of the nucleon probed with real and virtual photons, *Phys. Rev. D* 39 (1989) 3275.
- [12] W. Vogelsang, A. Vogt, Constraints on the proton's gluon distribution from prompt photon production, *Nucl. Phys. B* 453 (1995) 334, arXiv:hep-ph/9505404.
- [13] P. Aurenche, M. Fontannaz, J.Ph. Guillet, E. Pilon, M. Werlen, A new critical study of photon production in hadronic collisions, *Phys. Rev. D* 73 (2006) 094007, and references therein, arXiv:hep-ph/0602133.
- [14] R. Ichou, D. d'Enterria, Sensitivity of isolated photon production at TeV hadron colliders to the gluon distribution in the proton, *Phys. Rev. D* 82 (2010) 014015, and references therein, arXiv:1005.4529 [hep-ph].
- [15] D. d'Enterria, J. Rojo, Quantitative constraints on the gluon distribution function in the proton from collider isolated-photon data, *Nucl. Phys. B* 860 (2012) 311, and references therein, arXiv:1202.1762 [hep-ph].
- [16] L. Carminati, et al., Sensitivity of the LHC isolated- γ + jet data to the parton distribution functions of the proton, *Europhys. Lett.* 101 (2013) 61002, arXiv:1212.5511 [hep-ph].
- [17] ATLAS Collaboration, Measurement of the inclusive isolated prompt photon cross section in pp collisions at $\sqrt{s} = 7$ TeV with the ATLAS detector, *Phys. Rev. D* 83 (2011) 052005, arXiv:1012.4389 [hep-ex].
- [18] ATLAS Collaboration, Measurement of the inclusive isolated prompt photon cross-section in pp collisions at $\sqrt{s} = 7$ TeV using 35 pb^{-1} of ATLAS data, *Phys. Lett. B* 706 (2011) 150, arXiv:1108.0253 [hep-ex].
- [19] ATLAS Collaboration, Measurement of the inclusive isolated prompt photons cross section in pp collisions at $\sqrt{s} = 7$ TeV with the ATLAS detector using 4.6 fb^{-1} , *Phys. Rev. D* 89 (2014) 052004, arXiv:1311.1440 [hep-ex].
- [20] ATLAS Collaboration, Measurement of the inclusive isolated prompt photon cross section in pp collisions at $\sqrt{s} = 8$ TeV with the ATLAS detector, *J. High Energy Phys.* 1608 (2016) 005, arXiv:1605.03495 [hep-ex].
- [21] CMS Collaboration, Measurement of the isolated prompt photon production cross section in pp collisions at $\sqrt{s} = 7$ TeV, *Phys. Rev. Lett.* 106 (2011) 082001, arXiv:1012.0799 [hep-ex].
- [22] CMS Collaboration, Measurement of the differential cross section for isolated prompt photon production in pp collisions at 7 TeV, *Phys. Rev. D* 84 (2011) 052011, arXiv:1108.2044 [hep-ex].
- [23] ATLAS Collaboration, The ATLAS experiment at the CERN large hadron collider, *J. Instrum.* 3 (2008) S08003.
- [24] ATLAS Collaboration, ATLAS Insertable B-Layer Technical Design Report, ATLAS-TDR-19, 2010, url: <https://cds.cern.ch/record/1291633>.
- [25] ATLAS Collaboration, 2015 Start-Up Trigger Menu and Initial Performance Assessment of the ATLAS Trigger Using Run-2 Data, ATL-DAQ-PUB-2016-001, 2016, url: <https://cds.cern.ch/record/2136007>.
- [26] ATLAS Collaboration, Improved luminosity determination in pp collisions at $\sqrt{s} = 7$ TeV using the ATLAS detector at the LHC, *Eur. Phys. J. C* 73 (2013) 2518, arXiv:1302.4393 [hep-ex].
- [27] ATLAS Collaboration, Luminosity determination in pp collisions at $\sqrt{s} = 8$ TeV using the ATLAS detector at the LHC, *Eur. Phys. J. C* 76 (2016) 653, arXiv:1608.03953 [hep-ex].
- [28] ATLAS Collaboration, Measurement of the photon identification efficiencies with the ATLAS detector using LHC Run-1 data, *Eur. Phys. J. C* 76 (2016) 666, arXiv:1606.01813 [hep-ex].
- [29] ATLAS Collaboration, Photon Identification in 2015 ATLAS Data, ATL-PHYS-PUB-2016-014, 2016, url: <https://cds.cern.ch/record/2203125>.
- [30] ATLAS Collaboration, Electron and photon energy calibration with the ATLAS detector using LHC Run 1 data, *Eur. Phys. J. C* 74 (2014) 3071, arXiv:1407.5063 [hep-ex].
- [31] ATLAS Collaboration, Topological cell clustering in the ATLAS calorimeters and its performance in LHC Run 1, arXiv:1603.02934 [hep-ex], 2016.
- [32] M. Cacciari, G.P. Salam, G. Soyez, The catchment area of jets, *J. High Energy Phys.* 0804 (2008) 005, arXiv:0802.1188 [hep-ph].
- [33] M. Cacciari, G.P. Salam, S. Sapeta, On the characterisation of the underlying event, *J. High Energy Phys.* 1004 (2010) 065, arXiv:0912.4926 [hep-ph].
- [34] S.D. Ellis, D.E. Soper, Successive combination jet algorithm for hadron collisions, *Phys. Rev. D* 48 (1993) 3160.
- [35] S. Catani, Y.L. Dokshitzer, M.H. Seymour, B.R. Webber, Longitudinally invariant k_t clustering algorithms for hadron hadron collisions, *Nucl. Phys. B* 406 (1993) 187.
- [36] T. Sjöstrand, S. Mrenna, P.Z. Skands, A Brief Introduction to PYTHIA 8.1, *Comput. Phys. Commun.* 178 (2008) 852, arXiv:0710.3820 [hep-ph].
- [37] T. Gleisberg, et al., Event generation with SHERPA 1.1, *J. High Energy Phys.* 0902 (2009) 007, arXiv:0811.4622 [hep-ph].
- [38] B. Andersson, G. Gustafson, G. Ingelman, T. Sjöstrand, Parton fragmentation and string dynamics, *Phys. Rep.* 97 (1983) 31.
- [39] C. Winter, F. Krauss, G. Soff, A modified cluster hadronisation model, *Eur. Phys. J. C* 36 (2004) 381, arXiv:hep-ph/0311085.
- [40] R.D. Ball, et al., Parton distributions with LHC data, *Nucl. Phys. B* 867 (2013) 244, arXiv:1207.1303 [hep-ph].
- [41] H.-L. Lai, et al., New parton distributions for collider physics, *Phys. Rev. D* 82 (2010) 074024, arXiv:1007.2241 [hep-ph].
- [42] ATLAS Collaboration, ATLAS Run 1 Pythia8 Tunes, ATL-PHYS-PUB-2014-021, 2014, url: <https://cds.cern.ch/record/1966419>.
- [43] S. Agostinelli, et al., GEANT4 – a simulation toolkit, *Nucl. Instrum. Methods A* 506 (2003) 250.
- [44] ATLAS Collaboration, The ATLAS simulation infrastructure, *Eur. Phys. J. C* 70 (2010) 823, arXiv:1005.4568 [physics.ins-det].
- [45] ATLAS Collaboration, Summary of ATLAS Pythia 8 Tunes, ATL-PHYS-PUB-2012-003, 2012, url: <https://cds.cern.ch/record/1474107>.
- [46] ATLAS Collaboration, Measurement of the inelastic proton–proton cross-section at $\sqrt{s} = 7$ TeV with the ATLAS detector, *Nat. Commun.* 2 (2011) 463, arXiv:1104.0326 [hep-ex].
- [47] S. Höche, F. Krauss, S. Schumann, F. Siegert, QCD matrix elements and truncated showers, *J. High Energy Phys.* 0905 (2009) 053, arXiv:0903.1219 [hep-ph].
- [48] S. Frixione, Isolated photons in perturbative QCD, *Phys. Lett. B* 429 (1998) 369, arXiv:hep-ph/9801442.
- [49] S. Catani, M. Fontannaz, J.Ph. Guillet, E. Pilon, Cross section of isolated prompt photons in hadron–hadron collisions, *J. High Energy Phys.* 0205 (2002) 028, arXiv:hep-ph/0204023.
- [50] L.A. Harland-Lang, A.D. Martin, P. Motylinski, R.S. Thorne, Parton distributions in the LHC era: MMHT 2014 PDFs, *Eur. Phys. J. C* 75 (2015) 204, arXiv:1412.3989 [hep-ph].
- [51] L. Bourhis, M. Fontannaz, J.Ph. Guillet, Quark and gluon fragmentation functions into photons, *Eur. Phys. J. C* 2 (1998) 529, arXiv:hep-ph/9704447.
- [52] S. Dulat, et al., New parton distribution functions from a global analysis of quantum chromodynamics, *Phys. Rev. D* 93 (2016) 033006, arXiv:1506.07443 [hep-ph].
- [53] NNPDF Collaboration, R.D. Ball, et al., Parton distributions for the LHC Run II, *J. High Energy Phys.* 1504 (2015) 040, arXiv:1410.8849 [hep-ph].
- [54] ATLAS Collaboration, Measurement of the production cross section of an isolated photon associated with jets in proton–proton collisions at $\sqrt{s} = 7$ TeV with the ATLAS detector, *Phys. Rev. D* 85 (2012) 092014, arXiv:1203.3161 [hep-ex].
- [55] ATLAS Collaboration, Dynamics of isolated-photon plus jet production in pp collisions at $\sqrt{s} = 7$ TeV with the ATLAS detector, *Nucl. Phys. B* 875 (2013) 483, arXiv:1307.6795 [hep-ex].
- [56] G. D'Agostini, A multidimensional unfolding method based on Bayes' theorem, *Nucl. Instrum. Methods A* 362 (1995) 487.
- [57] J. Pumplin, et al., Uncertainties of predictions from parton distribution functions, 2: the Hessian method, *Phys. Rev. D* 65 (2001) 014013, arXiv:hep-ph/0101032.
- [58] P.M. Nadolsky, Z. Sullivan, PDF uncertainties in WH production at Tevatron, arXiv:hep-ph/0110378, 2001.
- [59] ATLAS Collaboration, ATLAS Computing Acknowledgements 2016–2017, ATL-GEN-PUB-2016-002, 2016, url: <https://cds.cern.ch/record/2202407>.

The ATLAS Collaboration

M. Aaboud^{137d}, G. Aad⁸⁸, B. Abbott¹¹⁵, J. Abdallah⁸, O. Abdinov¹², B. Abeloos¹¹⁹, S.H. Abidi¹⁶¹, O.S. AbouZeid¹³⁹, N.L. Abraham¹⁵¹, H. Abramowicz¹⁵⁵, H. Abreu¹⁵⁴, R. Abreu¹¹⁸, Y. Abulaiti^{148a,148b}, B.S. Acharya^{167a,167b,b}, S. Adachi¹⁵⁷, L. Adamczyk^{41a}, D.L. Adams²⁷, J. Adelman¹¹⁰, M. Adersberger¹⁰², T. Adaye¹³³, A.A. Affolder¹³⁹, T. Agatonovic-Jovin¹⁴, C. Agheorghiesei^{28b}, J.A. Aguilar-Saavedra^{128a,128f}, S.P. Ahlen²⁴, F. Ahmadov^{68,c}, G. Aielli^{135a,135b}, S. Akatsuka⁷¹, H. Akerstedt^{148a,148b}, T.P.A. Åkesson⁸⁴,

A.V. Akimov⁹⁸, G.L. Alberghi^{22a,22b}, J. Albert¹⁷², M.J. Alconada Verzini⁷⁴, M. Aleksa³²,
 I.N. Aleksandrov⁶⁸, C. Alexa^{28b}, G. Alexander¹⁵⁵, T. Alexopoulos¹⁰, M. Alhroob¹¹⁵, B. Ali¹³⁰,
 M. Aliev^{76a,76b}, G. Alimonti^{94a}, J. Alison³³, S.P. Alkire³⁸, B.M.M. Allbrooke¹⁵¹, B.W. Allen¹¹⁸,
 P.P. Allport¹⁹, A. Aloisio^{106a,106b}, A. Alonso³⁹, F. Alonso⁷⁴, C. Alpigiani¹⁴⁰, A.A. Alshehri⁵⁶, M. Alstamy⁸⁸,
 B. Alvarez Gonzalez³², D. Álvarez Piqueras¹⁷⁰, M.G. Alviggi^{106a,106b}, B.T. Amadio¹⁶,
 Y. Amaral Coutinho^{26a}, C. Amelung²⁵, D. Amidei⁹², S.P. Amor Dos Santos^{128a,128c}, A. Amorim^{128a,128b},
 S. Amoroso³², G. Amundsen²⁵, C. Anastopoulos¹⁴¹, L.S. Ancu⁵², N. Andari¹⁹, T. Andeen¹¹,
 C.F. Anders^{60b}, J.K. Anders⁷⁷, K.J. Anderson³³, A. Andreazza^{94a,94b}, V. Andrei^{60a}, S. Angelidakis⁹,
 I. Angelozzi¹⁰⁹, A. Angerami³⁸, F. Anghinolfi³², A.V. Anisenkov^{111,d}, N. Anjos¹³, A. Annovi^{126a,126b},
 C. Antel^{60a}, M. Antonelli⁵⁰, A. Antonov^{100,*}, D.J. Antrim¹⁶⁶, F. Anulli^{134a}, M. Aoki⁶⁹, L. Aperio Bella³²,
 G. Arabidze⁹³, Y. Arai⁶⁹, J.P. Araque^{128a}, V. Araujo Ferraz^{26a}, A.T.H. Arce⁴⁸, R.E. Ardell⁸⁰, F.A. Arduh⁷⁴,
 J-F. Arguin⁹⁷, S. Argyropoulos⁶⁶, M. Arik^{20a}, A.J. Armbruster¹⁴⁵, L.J. Armitage⁷⁹, O. Arnaez³²,
 H. Arnold⁵¹, M. Arratia³⁰, O. Arslan²³, A. Artamonov⁹⁹, G. Artoni¹²², S. Artz⁸⁶, S. Asai¹⁵⁷, N. Asbah⁴⁵,
 A. Ashkenazi¹⁵⁵, L. Asquith¹⁵¹, K. Assamagan²⁷, R. Astalos^{146a}, M. Atkinson¹⁶⁹, N.B. Atlay¹⁴³,
 K. Augsten¹³⁰, G. Avolio³², B. Axen¹⁶, M.K. Ayoub¹¹⁹, G. Azuelos^{97,e}, A.E. Baas^{60a}, M.J. Baca¹⁹,
 H. Bachacou¹³⁸, K. Bachas^{76a,76b}, M. Backes¹²², M. Backhaus³², P. Bagiachi^{134a,134b}, P. Bagnaia^{134a,134b},
 J.T. Baines¹³³, M. Bajic³⁹, O.K. Baker¹⁷⁹, E.M. Baldin^{111,d}, P. Balek¹⁷⁵, T. Balestri¹⁵⁰, F. Balli¹³⁸,
 W.K. Balunas¹²⁴, E. Banas⁴², Sw. Banerjee^{176,f}, A.A.E. Bannoura¹⁷⁸, L. Barak³², E.L. Barberio⁹¹,
 D. Barberis^{53a,53b}, M. Barbero⁸⁸, T. Barillari¹⁰³, M-S Barisits³², T. Barklow¹⁴⁵, N. Barlow³⁰,
 S.L. Barnes^{36c}, B.M. Barnett¹³³, R.M. Barnett¹⁶, Z. Barnovska-Blenessy^{36a}, A. Baroncelli^{136a}, G. Barone²⁵,
 A.J. Barr¹²², L. Barranco Navarro¹⁷⁰, F. Barreiro⁸⁵, J. Barreiro Guimarães da Costa^{35a}, R. Bartoldus¹⁴⁵,
 A.E. Barton⁷⁵, P. Bartos^{146a}, A. Basalae¹²⁵, A. Bassalat^{119,g}, R.L. Bates⁵⁶, S.J. Batista¹⁶¹, J.R. Batley³⁰,
 M. Battaglia¹³⁹, M. Bauce^{134a,134b}, F. Bauer¹³⁸, H.S. Bawa^{145,h}, J.B. Beacham¹¹³, M.D. Beattie⁷⁵,
 T. Beau⁸³, P.H. Beauchemin¹⁶⁵, P. Bechtel²³, H.P. Beck^{18,i}, K. Becker¹²², M. Becker⁸⁶, M. Beckingham¹⁷³,
 C. Becot¹¹², A.J. Beddall^{20e}, A. Beddall^{20b}, V.A. Bednyakov⁶⁸, M. Bedognetti¹⁰⁹, C.P. Bee¹⁵⁰,
 T.A. Beermann³², M. Begalli^{26a}, M. Begel²⁷, J.K. Behr⁴⁵, A.S. Bell⁸¹, G. Bella¹⁵⁵, L. Bellagamba^{22a},
 A. Bellerive³¹, M. Bellomo⁸⁹, K. Belotskiy¹⁰⁰, O. Beltramello³², N.L. Belyaev¹⁰⁰, O. Benary^{155,*},
 D. Bencheikroun^{137a}, M. Bender¹⁰², K. Bendtz^{148a,148b}, N. Benekos¹⁰, Y. Benhammou¹⁵⁵,
 E. Benhar Nocchioli¹⁷⁹, J. Benitez⁶⁶, D.P. Benjamin⁴⁸, M. Benoit⁵², J.R. Bensinger²⁵, S. Bentvelsen¹⁰⁹,
 L. Beresford¹²², M. Beretta⁵⁰, D. Berge¹⁰⁹, E. Bergeaas Kuutmann¹⁶⁸, N. Berger⁵, J. Beringer¹⁶,
 S. Berlendis⁵⁸, N.R. Bernard⁸⁹, G. Bernardi⁸³, C. Bernius¹¹², F.U. Bernlochner²³, T. Berry⁸⁰, P. Berta¹³¹,
 C. Bertella⁸⁶, G. Bertoli^{148a,148b}, F. Bertolucci^{126a,126b}, I.A. Bertram⁷⁵, C. Bertsche⁴⁵, D. Bertsche¹¹⁵,
 G.J. Besjes³⁹, O. Bessidskaia Bylund^{148a,148b}, M. Bessner⁴⁵, N. Besson¹³⁸, C. Betancourt⁵¹, A. Bethani⁸⁷,
 S. Bethke¹⁰³, A.J. Bevan⁷⁹, R.M. Bianchi¹²⁷, M. Bianco³², O. Biebel¹⁰², D. Biedermann¹⁷, R. Bielski⁸⁷,
 N.V. Biesuz^{126a,126b}, M. Biglietti^{136a}, J. Bilbao De Mendizabal⁵², T.R.V. Billoud⁹⁷, H. Bilokon⁵⁰,
 M. Bindi⁵⁷, A. Bingul^{20b}, C. Bini^{134a,134b}, S. Biondi^{22a,22b}, T. Bisanz⁵⁷, C. Bittrich⁴⁷, D.M. Bjergaard⁴⁸,
 C.W. Black¹⁵², J.E. Black¹⁴⁵, K.M. Black²⁴, D. Blackburn¹⁴⁰, R.E. Blair⁶, T. Blazek^{146a}, I. Bloch⁴⁵,
 C. Blocker²⁵, A. Blue⁵⁶, W. Blum^{86,*}, U. Blumenschein⁷⁹, S. Blunier^{34a}, G.J. Bobbink¹⁰⁹,
 V.S. Bobrovnikov^{111,d}, S.S. Bocchetta⁸⁴, A. Bocci⁴⁸, C. Bock¹⁰², M. Boehler⁵¹, D. Boerner¹⁷⁸,
 D. Bogavac¹⁰², A.G. Bogdanchikov¹¹¹, C. Bohm^{148a}, V. Boisvert⁸⁰, P. Bokan^{168,j}, T. Bold^{41a},
 A.S. Boldyrev¹⁰¹, M. Bomben⁸³, M. Bona⁷⁹, M. Boonekamp¹³⁸, A. Borisov¹³², G. Borissov⁷⁵,
 J. Bortfeldt³², D. Bortoletto¹²², V. Bortolotto^{62a,62b,62c}, K. Bos¹⁰⁹, D. Boscherini^{22a}, M. Bosman¹³,
 J.D. Bossio Sola²⁹, J. Boudreau¹²⁷, J. Bouffard², E.V. Bouhova-Thacker⁷⁵, D. Boumediene³⁷,
 C. Bourdarios¹¹⁹, S.K. Boutle⁵⁶, A. Boveia¹¹³, J. Boyd³², I.R. Boyko⁶⁸, J. Bracinik¹⁹, A. Brandt⁸,
 G. Brandt⁵⁷, O. Brandt^{60a}, U. Bratzler¹⁵⁸, B. Brau⁸⁹, J.E. Brau¹¹⁸, W.D. Breaden Madden⁵⁶,
 K. Brendlinger⁴⁵, A.J. Brennan⁹¹, L. Brenner¹⁰⁹, R. Brenner¹⁶⁸, S. Bressler¹⁷⁵, D.L. Briglin¹⁹,
 T.M. Bristow⁴⁹, D. Britton⁵⁶, D. Britzger⁴⁵, F.M. Brochu³⁰, I. Brock²³, R. Brock⁹³, G. Brooijmans³⁸,
 T. Brooks⁸⁰, W.K. Brooks^{34b}, J. Brosamer¹⁶, E. Brost¹¹⁰, J.H. Broughton¹⁹, P.A. Bruckman de Renstrom⁴²,
 D. Bruncko^{146b}, A. Bruni^{22a}, G. Bruni^{22a}, L.S. Bruni¹⁰⁹, BH Brunt³⁰, M. Bruschi^{22a}, N. Bruscino²³,
 P. Bryant³³, L. Bryngemark⁸⁴, T. Buanes¹⁵, Q. Buat¹⁴⁴, P. Buchholz¹⁴³, A.G. Buckley⁵⁶, I.A. Budagov⁶⁸,
 F. Buehrer⁵¹, M.K. Bugge¹²¹, O. Bulekov¹⁰⁰, D. Bullock⁸, H. Burckhart³², S. Burdin⁷⁷, C.D. Burgard⁵¹,
 A.M. Burger⁵, B. Burghgrave¹¹⁰, K. Burka⁴², S. Burke¹³³, I. Burmeister⁴⁶, J.T.P. Burr¹²², E. Busato³⁷,

D. Büscher⁵¹, V. Büscher⁸⁶, P. Bussey⁵⁶, J.M. Butler²⁴, C.M. Buttar⁵⁶, J.M. Butterworth⁸¹, P. Butti³²,
 W. Buttinger²⁷, A. Buzatu^{35c}, A.R. Buzykaev^{111,d}, S. Cabrera Urbán¹⁷⁰, D. Caforio¹³⁰, V.M. Cairo^{40a,40b},
 O. Cakir^{4a}, N. Calace⁵², P. Calafiura¹⁶, A. Calandri⁸⁸, G. Calderini⁸³, P. Calfayan⁶⁴, G. Callea^{40a,40b},
 L.P. Caloba^{26a}, S. Calvente Lopez⁸⁵, D. Calvet³⁷, S. Calvet³⁷, T.P. Calvet⁸⁸, R. Camacho Toro³³,
 S. Camarda³², P. Camarri^{135a,135b}, D. Cameron¹²¹, R. Caminal Armadans¹⁶⁹, C. Camincher⁵⁸,
 S. Campana³², M. Campanelli⁸¹, A. Camplani^{94a,94b}, A. Campoverde¹⁴³, V. Canale^{106a,106b},
 M. Cano Bret^{36c}, J. Cantero¹¹⁶, T. Cao¹⁵⁵, M.D.M. Capeans Garrido³², I. Caprini^{28b}, M. Caprini^{28b},
 M. Capua^{40a,40b}, R.M. Carbone³⁸, R. Cardarelli^{135a}, F. Cardillo⁵¹, I. Carli¹³¹, T. Carli³², G. Carlino^{106a},
 B.T. Carlson¹²⁷, L. Carminati^{94a,94b}, R.M.D. Carney^{148a,148b}, S. Caron¹⁰⁸, E. Carquin^{34b},
 G.D. Carrillo-Montoya³², J. Carvalho^{128a,128c}, D. Casadei¹⁹, M.P. Casado^{13,k}, M. Casolino¹³,
 D.W. Casper¹⁶⁶, R. Castelijin¹⁰⁹, A. Castelli¹⁰⁹, V. Castillo Gimenez¹⁷⁰, N.F. Castro^{128a,l}, A. Catinaccio³²,
 J.R. Catmore¹²¹, A. Cattai³², J. Caudron²³, V. Cavaliere¹⁶⁹, E. Cavallaro¹³, D. Cavalli^{94a},
 M. Cavalli-Sforza¹³, V. Cavasinni^{126a,126b}, E. Celebi^{20a}, F. Ceradini^{136a,136b}, L. Cerda Alberich¹⁷⁰,
 A.S. Cerqueira^{26b}, A. Cerri¹⁵¹, L. Cerrito^{135a,135b}, F. Cerutti¹⁶, A. Cervelli¹⁸, S.A. Cetin^{20d}, A. Chafaq^{137a},
 D. Chakraborty¹¹⁰, S.K. Chan⁵⁹, W.S. Chan¹⁰⁹, Y.L. Chan^{62a}, P. Chang¹⁶⁹, J.D. Chapman³⁰,
 D.G. Charlton¹⁹, A. Chatterjee⁵², C.C. Chau¹⁶¹, C.A. Chavez Barajas¹⁵¹, S. Che¹¹³, S. Cheatham^{167a,167c},
 A. Chegwidden⁹³, S. Chekanov⁶, S.V. Chekulaev^{163a}, G.A. Chelkov^{68,m}, M.A. Chelstowska³², C. Chen⁶⁷,
 H. Chen²⁷, S. Chen^{35b}, S. Chen¹⁵⁷, X. Chen^{35c,n}, Y. Chen⁷⁰, H.C. Cheng⁹², H.J. Cheng^{35a}, Y. Cheng³³,
 A. Cheplakov⁶⁸, E. Cheremushkina¹³², R. Cherkouki El Moursli^{137e}, V. Chernyatin^{27,*}, E. Cheu⁷,
 L. Chevalier¹³⁸, V. Chiarella⁵⁰, G. Chiarelli^{126a,126b}, G. Chiodini^{76a}, A.S. Chisholm³², A. Chitan^{28b},
 Y.H. Chiu¹⁷², M.V. Chizhov⁶⁸, K. Choi⁶⁴, A.R. Chomont³⁷, S. Chouridou⁹, B.K.B. Chow¹⁰²,
 V. Christodoulou⁸¹, D. Chromek-Burckhart³², M.C. Chu^{62a}, J. Chudoba¹²⁹, A.J. Chuinard⁹⁰,
 J.J. Chwastowski⁴², L. Chytka¹¹⁷, A.K. Ciftci^{4a}, D. Cinca⁴⁶, V. Cindro⁷⁸, I.A. Cioara²³, C. Ciocca^{22a,22b},
 A. Ciocio¹⁶, F. Ciotto^{106a,106b}, Z.H. Citron¹⁷⁵, M. Citterio^{94a}, M. Ciubancan^{28b}, A. Clark⁵², B.L. Clark⁵⁹,
 M.R. Clark³⁸, P.J. Clark⁴⁹, R.N. Clarke¹⁶, C. Clement^{148a,148b}, Y. Coadou⁸⁸, M. Cobal^{167a,167c},
 A. Coccaro⁵², J. Cochran⁶⁷, L. Colasurdo¹⁰⁸, B. Cole³⁸, A.P. Colijn¹⁰⁹, J. Collot⁵⁸, T. Colombo¹⁶⁶,
 P. Conde Muñio^{128a,128b}, E. Coniavitis⁵¹, S.H. Connell^{147b}, I.A. Connelly⁸⁷, V. Consorti⁵¹,
 S. Constantinescu^{28b}, G. Conti³², F. Conventi^{106a,o}, M. Cooke¹⁶, B.D. Cooper⁸¹, A.M. Cooper-Sarkar¹²²,
 F. Cormier¹⁷¹, K.J.R. Cormier¹⁶¹, T. Cornelissen¹⁷⁸, M. Corradi^{134a,134b}, F. Corriveau^{90,p},
 A. Cortes-Gonzalez³², G. Cortiana¹⁰³, G. Costa^{94a}, M.J. Costa¹⁷⁰, D. Costanzo¹⁴¹, G. Cottin³⁰,
 G. Cowan⁸⁰, B.E. Cox⁸⁷, K. Cranmer¹¹², S.J. Crawley⁵⁶, R.A. Creager¹²⁴, G. Cree³¹, S. Crépe-Renaudin⁵⁸,
 F. Crescioli⁸³, W.A. Cribbs^{148a,148b}, M. Crispin Ortuzar¹²², M. Cristinziani²³, V. Croft¹⁰⁸,
 G. Crosetti^{40a,40b}, A. Cueto⁸⁵, T. Cuhadar Donszelmann¹⁴¹, J. Cummings¹⁷⁹, M. Curatolo⁵⁰, J. Cúth⁸⁶,
 H. Czirr¹⁴³, P. Czodrowski³², G. D'amen^{22a,22b}, S. D'Auria⁵⁶, M. D'Onofrio⁷⁷,
 M.J. Da Cunha Sargedas De Sousa^{128a,128b}, C. Da Via⁸⁷, W. Dabrowski^{41a}, T. Dado^{146a}, T. Dai⁹²,
 O. Dale¹⁵, F. Dallaire⁹⁷, C. Dallapiccola⁸⁹, M. Dam³⁹, J.R. Dandoy¹²⁴, N.P. Dang⁵¹, A.C. Daniells¹⁹,
 N.S. Dann⁸⁷, M. Danninger¹⁷¹, M. Dano Hoffmann¹³⁸, V. Dao¹⁵⁰, G. Darbo^{53a}, S. Darmora⁸,
 J. Dassoulas³, A. Dattagupta¹¹⁸, T. Daubney⁴⁵, W. Davey²³, C. David⁴⁵, T. Davidek¹³¹, M. Davies¹⁵⁵,
 P. Davison⁸¹, E. Dawe⁹¹, I. Dawson¹⁴¹, K. De⁸, R. de Asmundis^{106a}, A. De Benedetti¹¹⁵,
 S. De Castro^{22a,22b}, S. De Cecco⁸³, N. De Groot¹⁰⁸, P. de Jong¹⁰⁹, H. De la Torre⁹³, F. De Lorenzi⁶⁷,
 A. De Maria⁵⁷, D. De Pedis^{134a}, A. De Salvo^{134a}, U. De Sanctis¹⁵¹, A. De Santo¹⁵¹,
 K. De Vasconcelos Corga⁸⁸, J.B. De Vivie De Regie¹¹⁹, W.J. Dearnaley⁷⁵, R. Debbé²⁷, C. Debenedetti¹³⁹,
 D.V. Dedovich⁶⁸, N. Dehghanian³, I. Deigaard¹⁰⁹, M. Del Gaudio^{40a,40b}, J. Del Peso⁸⁵,
 T. Del Prete^{126a,126b}, D. Delgove¹¹⁹, F. Deliot¹³⁸, C.M. Delitzsch⁵², A. Dell'Acqua³², L. Dell'Asta²⁴,
 M. Dell'Orso^{126a,126b}, M. Della Pietra^{106a,106b}, D. della Volpe⁵², M. Delmastro⁵, P.A. Delsart⁵⁸,
 D.A. DeMarco¹⁶¹, S. Demers¹⁷⁹, M. Demichev⁶⁸, A. Demilly⁸³, S.P. Denisov¹³², D. Denysiuk¹³⁸,
 D. Derendarz⁴², J.E. Derkaoui^{137d}, F. Derue⁸³, P. Dervan⁷⁷, K. Desch²³, C. Deterre⁴⁵, K. Dette⁴⁶,
 P.O. Deviveiros³², A. Dewhurst¹³³, S. Dhaliwal²⁵, A. Di Ciaccio^{135a,135b}, L. Di Ciaccio⁵,
 W.K. Di Clemente¹²⁴, C. Di Donato^{106a,106b}, A. Di Girolamo³², B. Di Girolamo³², B. Di Micco^{136a,136b},
 R. Di Nardo³², K.F. Di Petrillo⁵⁹, A. Di Simone⁵¹, R. Di Sipio¹⁶¹, D. Di Valentino³¹, C. Diaconu⁸⁸,
 M. Diamond¹⁶¹, F.A. Dias⁴⁹, M.A. Diaz^{34a}, E.B. Diehl⁹², J. Dietrich¹⁷, S. Díez Cornell⁴⁵,
 A. Dimitrievska¹⁴, J. Dingfelder²³, P. Dita^{28b}, S. Dita^{28b}, F. Dittus³², F. Djama⁸⁸, T. Djobava^{54b},

J.I. Djuvsland^{60a}, M.A.B. do Vale^{26c}, D. Dobos³², M. Dobre^{28b}, C. Doglioni⁸⁴, J. Dolejsi¹³¹, Z. Dolezal¹³¹, M. Donadelli^{26d}, S. Donati^{126a,126b}, P. Dondero^{123a,123b}, J. Donini³⁷, J. Dopke¹³³, A. Doria^{106a}, M.T. Dova⁷⁴, A.T. Doyle⁵⁶, E. Drechsler⁵⁷, M. Dris¹⁰, Y. Du^{36b}, J. Duarte-Campderros¹⁵⁵, E. Duchovni¹⁷⁵, G. Duckeck¹⁰², O.A. Ducu^{97,q}, D. Duda¹⁰⁹, A. Dudarev³², A. Chr. Dudder⁸⁶, E.M. Duffield¹⁶, L. Duflot¹¹⁹, M. Dührssen³², M. Dumancic¹⁷⁵, A.E. Dumitriu^{28b}, A.K. Duncan⁵⁶, M. Dunford^{60a}, H. Duran Yildiz^{4a}, M. Düren⁵⁵, A. Durglishvili^{54b}, D. Duschinger⁴⁷, B. Dutta⁴⁵, M. Dyndal⁴⁵, C. Eckardt⁴⁵, K.M. Ecker¹⁰³, R.C. Edgar⁹², T. Eifert³², G. Eigen¹⁵, K. Einsweiler¹⁶, T. Ekelof¹⁶⁸, M. El Kacimi^{137c}, V. Ellajosyula⁸⁸, M. Ellert¹⁶⁸, S. Elles⁵, F. Ellinghaus¹⁷⁸, A.A. Elliot¹⁷², N. Ellis³², J. Elmsheuser²⁷, M. Elsing³², D. Emeliyanov¹³³, Y. Enari¹⁵⁷, O.C. Endner⁸⁶, J.S. Ennis¹⁷³, J. Erdmann⁴⁶, A. Ereditato¹⁸, G. Ernis¹⁷⁸, M. Ernst²⁷, S. Errede¹⁶⁹, E. Ertel⁸⁶, M. Escalier¹¹⁹, H. Esch⁴⁶, C. Escobar¹²⁷, B. Esposito⁵⁰, A.I. Etienvre¹³⁸, E. Etzion¹⁵⁵, H. Evans⁶⁴, A. Ezhilov¹²⁵, F. Fabbri^{22a,22b}, L. Fabbri^{22a,22b}, G. Facini³³, R.M. Fakhrutdinov¹³², S. Falciano^{134a}, R.J. Falla⁸¹, J. Faltova³², Y. Fang^{35a}, M. Fanti^{94a,94b}, A. Farbin⁸, A. Farilla^{136a}, C. Farina¹²⁷, E.M. Farina^{123a,123b}, T. Farooque⁹³, S. Farrell¹⁶, S.M. Farrington¹⁷³, P. Farthouat³², F. Fassi^{137e}, P. Fassnacht³², D. Fassouliotis⁹, M. Fauci Giannelli⁸⁰, A. Favareto^{53a,53b}, W.J. Fawcett¹²², L. Fayard¹¹⁹, O.L. Fedin^{125,r}, W. Fedorko¹⁷¹, S. Feigl¹²¹, L. Felgioni⁸⁸, C. Feng^{36b}, E.J. Feng³², H. Feng⁹², A.B. Fenyuk¹³², L. Feremenga⁸, P. Fernandez Martinez¹⁷⁰, S. Fernandez Perez¹³, J. Ferrando⁴⁵, A. Ferrari¹⁶⁸, P. Ferrari¹⁰⁹, R. Ferrari^{123a}, D.E. Ferreira de Lima^{60b}, A. Ferrer¹⁷⁰, D. Ferrere⁵², C. Ferretti⁹², F. Fiedler⁸⁶, A. Filipčič⁷⁸, M. Filipuzzi⁴⁵, F. Filthaut¹⁰⁸, M. Fincke-Keeler¹⁷², K.D. Finelli¹⁵², M.C.N. Fiolhais^{128a,128c,s}, L. Fiorini¹⁷⁰, A. Fischer², C. Fischer¹³, J. Fischer¹⁷⁸, W.C. Fisher⁹³, N. Flaschel⁴⁵, I. Fleck¹⁴³, P. Fleischmann⁹², R.R.M. Fletcher¹²⁴, T. Flick¹⁷⁸, B.M. Flierl¹⁰², L.R. Flores Castillo^{62a}, M.J. Flowerdew¹⁰³, G.T. Forcolin⁸⁷, A. Formica¹³⁸, A. Forti⁸⁷, A.G. Foster¹⁹, D. Fournier¹¹⁹, H. Fox⁷⁵, S. Fracchia¹³, P. Francavilla⁸³, M. Franchini^{22a,22b}, D. Francis³², L. Franconi¹²¹, M. Franklin⁵⁹, M. Frate¹⁶⁶, M. Fraternali^{123a,123b}, D. Freeborn⁸¹, S.M. Fressard-Batranceanu³², B. Freund⁹⁷, D. Froidevaux³², J.A. Frost¹²², C. Fukunaga¹⁵⁸, E. Fullana Torregrosa⁸⁶, T. Fusayasu¹⁰⁴, J. Fuster¹⁷⁰, C. Gabaldon⁵⁸, O. Gabizon¹⁵⁴, A. Gabrielli^{22a,22b}, A. Gabrielli¹⁶, G.P. Gach^{41a}, S. Gadatsch³², S. Gadomski⁸⁰, G. Gagliardi^{53a,53b}, L.G. Gagnon⁹⁷, P. Gagnon⁶⁴, C. Galea¹⁰⁸, B. Galhardo^{128a,128c}, E.J. Gallas¹²², B.J. Gallop¹³³, P. Gallus¹³⁰, G. Galster³⁹, K.K. Gan¹¹³, S. Ganguly³⁷, J. Gao^{36a}, Y. Gao⁷⁷, Y.S. Gao^{145,h}, F.M. Garay Walls⁴⁹, C. García¹⁷⁰, J.E. García Navarro¹⁷⁰, M. Garcia-Sciveres¹⁶, R.W. Gardner³³, N. Garelli¹⁴⁵, V. Garonne¹²¹, A. Gascon Bravo⁴⁵, K. Gasnikova⁴⁵, C. Gatti⁵⁰, A. Gaudiello^{53a,53b}, G. Gaudio^{123a}, I.L. Gavrilenko⁹⁸, C. Gay¹⁷¹, G. Gaycken²³, E.N. Gazis¹⁰, C.N.P. Gee¹³³, M. Geisen⁸⁶, M.P. Geisler^{60a}, K. Gellerstedt^{148a,148b}, C. Gemme^{53a}, M.H. Genest⁵⁸, C. Geng^{36a,t}, S. Gentile^{134a,134b}, C. Gentsos¹⁵⁶, S. George⁸⁰, D. Gerbaudo¹³, A. Gershon¹⁵⁵, S. Ghasemi¹⁴³, M. Ghneimat²³, B. Giacobbe^{22a}, S. Giagu^{134a,134b}, P. Giannetti^{126a,126b}, S.M. Gibson⁸⁰, M. Gignac¹⁷¹, M. Gilchriese¹⁶, D. Gillberg³¹, G. Gilles¹⁷⁸, D.M. Gingrich^{3,e}, N. Giokaris^{9,*}, M.P. Giordani^{167a,167c}, F.M. Giorgi^{22a}, P.F. Giraud¹³⁸, P. Giromini⁵⁹, D. Giugni^{94a}, F. Giuli¹²², C. Giuliani¹⁰³, M. Giulini^{60b}, B.K. Gjelsten¹²¹, S. Gkaitatzis¹⁵⁶, I. Gkialas⁹, E.L. Gkougkousis¹³⁹, L.K. Gladilin¹⁰¹, C. Glasman⁸⁵, J. Glatzer¹³, P.C.F. Glaysher⁴⁵, A. Glazov⁴⁵, M. Goblirsch-Kolb²⁵, J. Godlewski⁴², S. Goldfarb⁹¹, T. Golling⁵², D. Golubkov¹³², A. Gomes^{128a,128b,128d}, R. Gonçalo^{128a}, R. Goncalves Gama^{26a}, J. Goncalves Pinto Firmino Da Costa¹³⁸, G. Gonella⁵¹, L. Gonella¹⁹, A. Gongadze⁶⁸, S. González de la Hoz¹⁷⁰, S. Gonzalez-Sevilla⁵², L. Goossens³², P.A. Gorbounov⁹⁹, H.A. Gordon²⁷, I. Gorelov¹⁰⁷, B. Gorini³², E. Gorini^{76a,76b}, A. Gorišek⁷⁸, A.T. Goshaw⁴⁸, C. Gössling⁴⁶, M.I. Gostkin⁶⁸, C.R. Goudet¹¹⁹, D. Goujdami^{137c}, A.G. Goussiou¹⁴⁰, N. Govender^{147b,u}, E. Gozani¹⁵⁴, L. Graber⁵⁷, I. Grabowska-Bold^{41a}, P.O.J. Gradin⁵⁸, J. Gramling⁵², E. Gramstad¹²¹, S. Grancagnolo¹⁷, V. Gratchev¹²⁵, P.M. Gravila^{28f}, H.M. Gray³², Z.D. Greenwood^{82,v}, C. Grefe²³, K. Gregersen⁸¹, I.M. Gregor⁴⁵, P. Grenier¹⁴⁵, K. Grevtsov⁵, J. Griffiths⁸, A.A. Grillo¹³⁹, K. Grimm⁷⁵, S. Grinstein^{13,w}, Ph. Gris³⁷, J.-F. Grivaz¹¹⁹, S. Groh⁸⁶, E. Gross¹⁷⁵, J. Grosse-Knetter⁵⁷, G.C. Grossi⁸², Z.J. Grout⁸¹, L. Guan⁹², W. Guan¹⁷⁶, J. Guenther⁶⁵, F. Guescini^{163a}, D. Guest¹⁶⁶, O. Gueta¹⁵⁵, B. Gui¹¹³, E. Guido^{53a,53b}, T. Guillemin⁵, S. Guindon², U. Gul⁵⁶, C. Gumpert³², J. Guo^{36c}, W. Guo⁹², Y. Guo^{36a}, R. Gupta⁴³, S. Gupta¹²², G. Gustavino^{134a,134b}, P. Gutierrez¹¹⁵, N.G. Gutierrez Ortiz⁸¹, C. Gutschow⁸¹, C. Guyot¹³⁸, M.P. Guzik^{41a}, C. Gwenlan¹²², C.B. Gwilliam⁷⁷, A. Haas¹¹², C. Haber¹⁶, H.K. Hadavand⁸, A. Hadeef⁸⁸, S. Hageböck²³, M. Hagihara¹⁶⁴, H. Hakobyan^{180,*}, M. Haleem⁴⁵, J. Haley¹¹⁶, G. Halladjian⁹³, G.D. Hallewell⁸⁸, K. Hamacher¹⁷⁸, P. Hamal¹¹⁷, K. Hamano¹⁷², A. Hamilton^{147a},

G.N. Hamity¹⁴¹, P.G. Hamnett⁴⁵, L. Han^{36a}, S. Han^{35a}, K. Hanagaki^{69,x}, K. Hanawa¹⁵⁷, M. Hance¹³⁹, B. Haney¹²⁴, P. Hanke^{60a}, R. Hanna¹³⁸, J.B. Hansen³⁹, J.D. Hansen³⁹, M.C. Hansen²³, P.H. Hansen³⁹, K. Hara¹⁶⁴, A.S. Hard¹⁷⁶, T. Harenberg¹⁷⁸, F. Hariri¹¹⁹, S. Harkusha⁹⁵, R.D. Harrington⁴⁹, P.F. Harrison¹⁷³, F. Hartjes¹⁰⁹, N.M. Hartmann¹⁰², M. Hasegawa⁷⁰, Y. Hasegawa¹⁴², A. Hasib⁴⁹, S. Hassani¹³⁸, S. Haug¹⁸, R. Hauser⁹³, L. Hauswald⁴⁷, L.B. Havener³⁸, M. Havranek¹³⁰, C.M. Hawkes¹⁹, R.J. Hawking³², D. Hayakawa¹⁵⁹, D. Hayden⁹³, C.P. Hays¹²², J.M. Hays⁷⁹, H.S. Hayward⁷⁷, S.J. Haywood¹³³, S.J. Head¹⁹, T. Heck⁸⁶, V. Hedberg⁸⁴, L. Heelan⁸, K.K. Heidegger⁵¹, S. Heim⁴⁵, T. Heim¹⁶, B. Heinemann^{45,y}, J.J. Heinrich¹⁰², L. Heinrich¹¹², C. Heinz⁵⁵, J. Hejbal¹²⁹, L. Helary³², A. Held¹⁷¹, S. Hellman^{148a,148b}, C. Hensens³², J. Henderson¹²², R.C.W. Henderson⁷⁵, Y. Heng¹⁷⁶, S. Henkelmann¹⁷¹, A.M. Henriques Correia³², S. Henrot-Versille¹¹⁹, G.H. Herbert¹⁷, H. Herde²⁵, V. Herget¹⁷⁷, Y. Hernández Jiménez^{147c}, G. Herten⁵¹, R. Hertenberger¹⁰², L. Hervas³², T.C. Herwig¹²⁴, G.G. Hesketh⁸¹, N.P. Hessey^{163a}, J.W. Hetherly⁴³, S. Higashino⁶⁹, E. Higón-Rodríguez¹⁷⁰, E. Hill¹⁷², J.C. Hill³⁰, K.H. Hiller⁴⁵, S.J. Hillier¹⁹, I. Hinchliffe¹⁶, M. Hirose⁵¹, D. Hirschbuehl¹⁷⁸, B. Hiti⁷⁸, O. Hladik¹²⁹, X. Hoad⁴⁹, J. Hobbs¹⁵⁰, N. Hod^{163a}, M.C. Hodgkinson¹⁴¹, P. Hodgson¹⁴¹, A. Hoecker³², M.R. Hoferkamp¹⁰⁷, F. Hoenic¹⁰², D. Hohn²³, T.R. Holmes¹⁶, M. Homann⁴⁶, S. Honda¹⁶⁴, T. Honda⁶⁹, T.M. Hong¹²⁷, B.H. Hooberman¹⁶⁹, W.H. Hopkins¹¹⁸, Y. Horii¹⁰⁵, A.J. Horton¹⁴⁴, J-Y. Hostachy⁵⁸, S. Hou¹⁵³, A. Hoummada^{137a}, J. Howarth⁴⁵, J. Hoya⁷⁴, M. Hrabovsky¹¹⁷, I. Hristova¹⁷, J. Hrivnac¹¹⁹, T. Hryn'ova⁵, A. Hrynevich⁹⁶, P.J. Hsu⁶³, S.-C. Hsu¹⁴⁰, Q. Hu^{36a}, S. Hu^{36c}, Y. Huang^{35a}, Z. Hubacek¹³⁰, F. Hubaut⁸⁸, F. Huegging²³, T.B. Huffman¹²², E.W. Hughes³⁸, G. Hughes⁷⁵, M. Huhtinen³², P. Huo¹⁵⁰, N. Huseynov^{68,c}, J. Huston⁹³, J. Huth⁵⁹, G. Iacobucci⁵², G. Iakovidis²⁷, I. Ibragimov¹⁴³, L. Iconomidou-Fayard¹¹⁹, P. Iengo³², O. Igonkina^{109,z}, T. Iizawa¹⁷⁴, Y. Ikegami⁶⁹, M. Ikeno⁶⁹, Y. Ilchenko^{11,aa}, D. Iliadis¹⁵⁶, N. Ilic¹⁴⁵, G. Introzzi^{123a,123b}, P. Ioannou^{9,*}, M. Iodice^{136a}, K. Iordanidou³⁸, V. Ippolito⁵⁹, N. Ishijima¹²⁰, M. Ishino¹⁵⁷, M. Ishitsuka¹⁵⁹, C. Issever¹²², S. Istin^{20a}, F. Ito¹⁶⁴, J.M. Iturbe Ponce⁸⁷, R. Iuppa^{162a,162b}, H. Iwasaki⁶⁹, J.M. Izen⁴⁴, V. Izzo^{106a}, S. Jabbar³, P. Jackson¹, V. Jain², K.B. Jakobi⁸⁶, K. Jakobs⁵¹, S. Jakobsen³², T. Jakoubek¹²⁹, D.O. Jamin¹¹⁶, D.K. Jana⁸², R. Jansky⁶⁵, J. Janssen²³, M. Janus⁵⁷, P.A. Janus^{41a}, G. Jarlskog⁸⁴, N. Javadov^{68,c}, T. Javůrek⁵¹, M. Javurkova⁵¹, F. Jeanneau¹³⁸, L. Jeanty¹⁶, J. Jejelava^{54a,ab}, A. Jelinskas¹⁷³, P. Jenni^{51,ac}, C. Jeske¹⁷³, S. Jézéquel⁵, H. Ji¹⁷⁶, J. Jia¹⁵⁰, H. Jiang⁶⁷, Y. Jiang^{36a}, Z. Jiang¹⁴⁵, S. Jiggins⁸¹, J. Jimenez Pena¹⁷⁰, S. Jin^{35a}, A. Jinaru^{28b}, O. Jinnouchi¹⁵⁹, H. Jivan^{147c}, P. Johansson¹⁴¹, K.A. Johns⁷, C.A. Johnson⁶⁴, W.J. Johnson¹⁴⁰, K. Jon-And^{148a,148b}, R.W.L. Jones⁷⁵, S. Jones⁷, T.J. Jones⁷⁷, J. Jongmanns^{60a}, P.M. Jorge^{128a,128b}, J. Jovicevic^{163a}, X. Ju¹⁷⁶, A. Juste Rozas^{13,w}, M.K. Köhler¹⁷⁵, A. Kaczmarska⁴², M. Kado¹¹⁹, H. Kagan¹¹³, M. Kagan¹⁴⁵, S.J. Kahn⁸⁸, T. Kaji¹⁷⁴, E. Kajomovitz⁴⁸, C.W. Kalderon⁸⁴, A. Kaluza⁸⁶, S. Kama⁴³, A. Kamenshchikov¹³², N. Kanaya¹⁵⁷, S. Kaneti³⁰, L. Kanjir⁷⁸, V.A. Kantserov¹⁰⁰, J. Kanzaki⁶⁹, B. Kaplan¹¹², L.S. Kaplan¹⁷⁶, D. Kar^{147c}, K. Karakostas¹⁰, N. Karastathis¹⁰, M.J. Kareem⁵⁷, E. Karentzos¹⁰, S.N. Karpov⁶⁸, Z.M. Karpova⁶⁸, K. Karthik¹¹², V. Kartvelishvili⁷⁵, A.N. Karyukhin¹³², K. Kasahara¹⁶⁴, L. Kashif¹⁷⁶, R.D. Kass¹¹³, A. Kastanas¹⁴⁹, Y. Kataoka¹⁵⁷, C. Kato¹⁵⁷, A. Katre⁵², J. Katzy⁴⁵, K. Kawade¹⁰⁵, K. Kawagoe⁷³, T. Kawamoto¹⁵⁷, G. Kawamura⁵⁷, E.F. Kay⁷⁷, V.F. Kazanin^{111,d}, R. Keeler¹⁷², R. Kehoe⁴³, J.S. Keller⁴⁵, J.J. Kempster⁸⁰, H. Keoshkerian¹⁶¹, O. Kepka¹²⁹, B.P. Kerševan⁷⁸, S. Kersten¹⁷⁸, R.A. Keyes⁹⁰, M. Khader¹⁶⁹, F. Khalil-zada¹², A. Khanov¹¹⁶, A.G. Kharlamov^{111,d}, T. Kharlamova^{111,d}, A. Khodinov¹⁶⁰, T.J. Khoo⁵², V. Khovanskiy^{99,*}, E. Khramov⁶⁸, J. Khubua^{54b,ad}, S. Kido⁷⁰, C.R. Kilby⁸⁰, H.Y. Kim⁸, S.H. Kim¹⁶⁴, Y.K. Kim³³, N. Kimura¹⁵⁶, O.M. Kind¹⁷, B.T. King⁷⁷, D. Kirchmeier⁴⁷, J. Kirk¹³³, A.E. Kiryunin¹⁰³, T. Kishimoto¹⁵⁷, D. Kisielewska^{41a}, K. Kiuchi¹⁶⁴, O. Kivernyk¹³⁸, E. Kladiva^{146b}, T. Klapdor-Kleingrothaus⁵¹, M.H. Klein³⁸, M. Klein⁷⁷, U. Klein⁷⁷, K. Kleinknecht⁸⁶, P. Klimek¹¹⁰, A. Klimentov²⁷, R. Klingenberg⁴⁶, T. Klioutchnikova³², E.-E. Kluge^{60a}, P. Kluit¹⁰⁹, S. Kluth¹⁰³, J. Knapik⁴², E. Kneringer⁶⁵, E.B.F.G. Knoops⁸⁸, A. Knue¹⁰³, A. Kobayashi¹⁵⁷, D. Kobayashi¹⁵⁹, T. Kobayashi¹⁵⁷, M. Kobel⁴⁷, M. Kocian¹⁴⁵, P. Kodys¹³¹, T. Koffas³¹, E. Koffeman¹⁰⁹, N.M. Köhler¹⁰³, T. Koi¹⁴⁵, M. Kolb^{60b}, I. Koletsou⁵, A.A. Komar^{98,*}, Y. Komori¹⁵⁷, T. Kondo⁶⁹, N. Kondrashova^{36c}, K. Köneke⁵¹, A.C. König¹⁰⁸, T. Kono^{69,ae}, R. Konoplich^{112,af}, N. Konstantinidis⁸¹, R. Kopeliansky⁶⁴, S. Koperny^{41a}, A.K. Kopp⁵¹, K. Korcyl⁴², K. Kordas¹⁵⁶, A. Korn⁸¹, A.A. Korol^{111,d}, I. Korolkov¹³, E.V. Korolkova¹⁴¹, O. Kortner¹⁰³, S. Kortner¹⁰³, T. Kosek¹³¹, V.V. Kostyukhin²³, A. Kotwal⁴⁸, A. Koulouris¹⁰, A. Kourkoumeli-Charalampidi^{123a,123b}, C. Kourkoumelis⁹, V. Kouskoura²⁷,

A.B. Kowalewska⁴², R. Kowalewski¹⁷², T.Z. Kowalski^{41a}, C. Kozakai¹⁵⁷, W. Kozanecki¹³⁸, A.S. Kozhin¹³²,
 V.A. Kramarenko¹⁰¹, G. Kramberger⁷⁸, D. Krasnopevtsev¹⁰⁰, M.W. Krasny⁸³, A. Krasznahorkay³²,
 D. Krauss¹⁰³, A. Kravchenko²⁷, J.A. Kremer^{41a}, M. Kretz^{60c}, J. Kretzschmar⁷⁷, K. Kreutzfeldt⁵⁵,
 P. Krieger¹⁶¹, K. Krizka³³, K. Kroeninger⁴⁶, H. Kroha¹⁰³, J. Kroll¹²⁴, J. Kroseberg²³, J. Krstic¹⁴,
 U. Kruchonak⁶⁸, H. Krüger²³, N. Krumnack⁶⁷, M.C. Kruse⁴⁸, M. Kruskal²⁴, T. Kubota⁹¹, H. Kucuk⁸¹,
 S. Kудay^{4b}, J.T. Kuechler¹⁷⁸, S. Kuehn⁵¹, A. Kugel^{60c}, F. Kuger¹⁷⁷, T. Kuhl⁴⁵, V. Kukhtin⁶⁸, R. Kukla⁸⁸,
 Y. Kulchitsky⁹⁵, S. Kuleshov^{34b}, Y.P. Kulinich¹⁶⁹, M. Kuna^{134a,134b}, T. Kunigo⁷¹, A. Kupco¹²⁹,
 O. Kuprash¹⁵⁵, H. Kurashige⁷⁰, L.L. Kurchaninov^{163a}, Y.A. Kurochkin⁹⁵, M.G. Kurth^{35a}, V. Kus¹²⁹,
 E.S. Kuwertz¹⁷², M. Kuze¹⁵⁹, J. Kvita¹¹⁷, T. Kwan¹⁷², D. Kyriazopoulos¹⁴¹, A. La Rosa¹⁰³,
 J.L. La Rosa Navarro^{26d}, L. La Rotonda^{40a,40b}, C. Lacasta¹⁷⁰, F. Lacava^{134a,134b}, J. Lacey⁴⁵, H. Lacker¹⁷,
 D. Lacour⁸³, E. Ladygin⁶⁸, R. Lafaye⁵, B. Laforge⁸³, T. Lagouri¹⁷⁹, S. Lai⁵⁷, S. Lammers⁶⁴, W. Lampl⁷,
 E. Lançon²⁷, U. Landgraf⁵¹, M.P.J. Landon⁷⁹, M.C. Lanfermann⁵², V.S. Lang^{60a}, J.C. Lange¹³,
 A.J. Lankford¹⁶⁶, F. Lanni²⁷, K. Lantsch²³, A. Lanza^{123a}, A. Lapertosa^{53a,53b}, S. Laplace⁸³, J.F. Laporte¹³⁸,
 T. Lari^{94a}, F. Lasagni Manghi^{22a,22b}, M. Lassnig³², P. Laurelli⁵⁰, W. Lavrijsen¹⁶, A.T. Law¹³⁹, P. Laycock⁷⁷,
 T. Lazovich⁵⁹, M. Lazzaroni^{94a,94b}, B. Le⁹¹, O. Le Dortz⁸³, E. Le Guirriec⁸⁸, E.P. Le Quilleuc¹³⁸,
 M. LeBlanc¹⁷², T. LeCompte⁶, F. Ledroit-Guillon⁵⁸, C.A. Lee²⁷, S.C. Lee¹⁵³, L. Lee¹, B. Lefebvre⁹⁰,
 G. Lefebvre⁸³, M. Lefebvre¹⁷², F. Legger¹⁰², C. Leggett¹⁶, A. Lehan⁷⁷, G. Lehmann Miotto³², X. Lei⁷,
 W.A. Leight⁴⁵, A.G. Leister¹⁷⁹, M.A.L. Leite^{26d}, R. Leitner¹³¹, D. Lellouch¹⁷⁵, B. Lemmer⁵⁷, K.J.C. Leney⁸¹,
 T. Lenz²³, B. Lenzi³², R. Leone⁷, S. Leone^{126a,126b}, C. Leonidopoulos⁴⁹, G. Lerner¹⁵¹, C. Leroy⁹⁷,
 A.A.J. Lesage¹³⁸, C.G. Lester³⁰, M. Levchenko¹²⁵, J. Levêque⁵, D. Levin⁹², L.J. Levinson¹⁷⁵, M. Levy¹⁹,
 D. Lewis⁷⁹, M. Leyton⁴⁴, B. Li^{36a,t}, C. Li^{36a}, H. Li¹⁵⁰, L. Li⁴⁸, L. Li^{36c}, Q. Li^{35a}, S. Li⁴⁸, X. Li^{36c}, Y. Li¹⁴³,
 Z. Liang^{35a}, B. Liberti^{135a}, A. Liblong¹⁶¹, K. Lie¹⁶⁹, J. Liebal²³, W. Liebig¹⁵, A. Limosani¹⁵², S.C. Lin^{153,ag},
 T.H. Lin⁸⁶, B.E. Lindquist¹⁵⁰, A.E. Lioni⁵², E. Lipeles¹²⁴, A. Lipniacka¹⁵, M. Lisovsky^{60b}, T.M. Liss¹⁶⁹,
 A. Lister¹⁷¹, A.M. Litke¹³⁹, B. Liu^{153,ah}, H. Liu⁹², H. Liu²⁷, J. Liu^{36b}, J.B. Liu^{36a}, K. Liu⁸⁸, L. Liu¹⁶⁹,
 M. Liu^{36a}, Y.L. Liu^{36a}, Y. Liu^{36a}, M. Livan^{123a,123b}, A. Lleres⁵⁸, J. Llorente Merino^{35a}, S.L. Lloyd⁷⁹,
 C.Y. Lo^{62b}, F. Lo Sterzo¹⁵³, E.M. Lobodzinska⁴⁵, P. Loch⁷, F.K. Loebinger⁸⁷, K.M. Loew²⁵, A. Loginov^{179,*},
 T. Lohse¹⁷, K. Lohwasser⁴⁵, M. Lokajicek¹²⁹, B.A. Long²⁴, J.D. Long¹⁶⁹, R.E. Long⁷⁵, L. Longo^{76a,76b},
 K.A. Looper¹¹³, J.A. Lopez^{34b}, D. Lopez Mateos⁵⁹, I. Lopez Paz¹³, A. Lopez Solis⁸³, J. Lorenz¹⁰²,
 N. Lorenzo Martinez⁶⁴, M. Losada²¹, P.J. Lösel¹⁰², X. Lou^{35a}, A. Lounis¹¹⁹, J. Love⁶, P.A. Love⁷⁵,
 H. Lu^{62a}, N. Lu⁹², Y.J. Lu⁶³, H.J. Lubatti¹⁴⁰, C. Luci^{134a,134b}, A. Lucotte⁵⁸, C. Luedtke⁵¹, F. Luehring⁶⁴,
 W. Lukas⁶⁵, L. Luminari^{134a}, O. Lundberg^{148a,148b}, B. Lund-Jensen¹⁴⁹, P.M. Luzi⁸³, D. Lynn²⁷,
 R. Lysak¹²⁹, E. Lytken⁸⁴, V. Lyubushkin⁶⁸, H. Ma²⁷, L.L. Ma^{36b}, Y. Ma^{36b}, G. Maccarrone⁵⁰,
 A. Macchiolo¹⁰³, C.M. Macdonald¹⁴¹, B. Maček⁷⁸, J. Machado Miguens^{124,128b}, D. Madaffari⁸⁸,
 R. Madar³⁷, H.J. Maddocks¹⁶⁸, W.F. Mader⁴⁷, A. Madsen⁴⁵, J. Maeda⁷⁰, S. Maeland¹⁵, T. Maeno²⁷,
 A. Maeviskiy¹⁰¹, E. Magradze⁵⁷, J. Mahlstedt¹⁰⁹, C. Maiani¹¹⁹, C. Maidantchik^{26a}, A.A. Maier¹⁰³,
 T. Maier¹⁰², A. Maio^{128a,128b,128d}, S. Majewski¹¹⁸, Y. Makida⁶⁹, N. Makovec¹¹⁹, B. Malaescu⁸³,
 Pa. Malecki⁴², V.P. Maleev¹²⁵, F. Malek⁵⁸, U. Mallik⁶⁶, D. Malon⁶, C. Malone³⁰, S. Maltezos¹⁰,
 S. Malyukov³², J. Mamuzic¹⁷⁰, G. Mancini⁵⁰, L. Mandelli^{94a}, I. Mandić⁷⁸, J. Maneira^{128a,128b},
 L. Manhaes de Andrade Filho^{26b}, J. Manjarres Ramos^{163b}, A. Mann¹⁰², A. Manousos³², B. Mansoulie¹³⁸,
 J.D. Mansour^{35a}, R. Mantifel⁹⁰, M. Mantoani⁵⁷, S. Manzoni^{94a,94b}, L. Mapelli³², G. Marceca²⁹,
 L. March⁵², G. Marchiori⁸³, M. Marcisovsky¹²⁹, M. Marjanovic³⁷, D.E. Marley⁹², F. Marroquim^{26a},
 S.P. Marsden⁸⁷, Z. Marshall¹⁶, M.U.F. Martensson¹⁶⁸, S. Marti-Garcia¹⁷⁰, C.B. Martin¹¹³, T.A. Martin¹⁷³,
 V.J. Martin⁴⁹, B. Martin dit Latour¹⁵, M. Martinez^{13,w}, V.I. Martinez Outschoorn¹⁶⁹, S. Martin-Haugh¹³³,
 V.S. Martoiu^{28b}, A.C. Martyniuk⁸¹, A. Marzin¹¹⁵, L. Masetti⁸⁶, T. Mashimo¹⁵⁷, R. Mashinistov⁹⁸,
 J. Masik⁸⁷, A.L. Maslennikov^{111,d}, L. Massa^{135a,135b}, P. Mastrandrea⁵, A. Mastroberardino^{40a,40b},
 T. Masubuchi¹⁵⁷, P. Mättig¹⁷⁸, J. Maurer^{28b}, S.J. Maxfield⁷⁷, D.A. Maximov^{111,d}, R. Mazini¹⁵³,
 I. Maznas¹⁵⁶, S.M. Mazza^{94a,94b}, N.C. Mc Fadden¹⁰⁷, G. Mc Goldrick¹⁶¹, S.P. Mc Kee⁹², A. McCarn⁹²,
 R.L. McCarthy¹⁵⁰, T.G. McCarthy¹⁰³, L.I. McClymont⁸¹, E.F. McDonald⁹¹, J.A. Mcfayden⁸¹,
 G. Mchedlidze⁵⁷, S.J. McMahon¹³³, P.C. McNamara⁹¹, R.A. McPherson^{172,p}, S. Meehan¹⁴⁰, T.J. Megy⁵¹,
 S. Mehlhase¹⁰², A. Mehta⁷⁷, T. Meideck⁵⁸, K. Meier^{60a}, C. Meineck¹⁰², B. Meirose⁴⁴, D. Melini^{170,ai},
 B.R. Mellado Garcia^{147c}, M. Melo^{146a}, F. Meloni¹⁸, S.B. Menary⁸⁷, L. Meng⁷⁷, X.T. Meng⁹²,
 A. Mengarelli^{22a,22b}, S. Menke¹⁰³, E. Meoni¹⁶⁵, S. Mergelmeyer¹⁷, P. Mermod⁵², L. Merola^{106a,106b},

C. Meroni^{94a}, F.S. Merritt³³, A. Messina^{134a,134b}, J. Metcalfe⁶, A.S. Mete¹⁶⁶, C. Meyer¹²⁴, J.-P. Meyer¹³⁸, J. Meyer¹⁰⁹, H. Meyer Zu Theenhausen^{60a}, F. Miano¹⁵¹, R.P. Middleton¹³³, S. Miglioranza^{53a,53b}, L. Mijović⁴⁹, G. Mikenberg¹⁷⁵, M. Mikesikova¹²⁹, M. Mikuž⁷⁸, M. Milesi⁹¹, A. Milic²⁷, D.W. Miller³³, C. Mills⁴⁹, A. Milov¹⁷⁵, D.A. Milstead^{148a,148b}, A.A. Minaenko¹³², Y. Minami¹⁵⁷, I.A. Minashvili⁶⁸, A.I. Mincer¹¹², B. Mindur^{41a}, M. Mineev⁶⁸, Y. Minegishi¹⁵⁷, Y. Ming¹⁷⁶, L.M. Mir¹³, K.P. Mistry¹²⁴, T. Mitani¹⁷⁴, J. Mitrevski¹⁰², V.A. Mitsou¹⁷⁰, A. Miucci¹⁸, P.S. Miyagawa¹⁴¹, A. Mizukami⁶⁹, J.U. Mjörnmark⁸⁴, M. Mlynarikova¹³¹, T. Moa^{148a,148b}, K. Mochizuki⁹⁷, P. Mogg⁵¹, S. Mohapatra³⁸, S. Molander^{148a,148b}, R. Moles-Valls²³, R. Monden⁷¹, M.C. Mondragon⁹³, K. Mönig⁴⁵, J. Monk³⁹, E. Monnier⁸⁸, A. Montalbano¹⁵⁰, J. Montejo Berlingen³², F. Monticelli⁷⁴, S. Monzani^{94a,94b}, R.W. Moore³, N. Morange¹¹⁹, D. Moreno²¹, M. Moreno Llacer⁵⁷, P. Morettini^{53a}, S. Morgenstern³², D. Mori¹⁴⁴, T. Mori¹⁵⁷, M. Morii⁵⁹, M. Morinaga¹⁵⁷, V. Morisbak¹²¹, A.K. Morley¹⁵², G. Mornacchi³², J.D. Morris⁷⁹, L. Morvaj¹⁵⁰, P. Moschovakos¹⁰, M. Mosidze^{54b}, H.J. Moss¹⁴¹, J. Moss^{145,aj}, K. Motohashi¹⁵⁹, R. Mount¹⁴⁵, E. Mountricha²⁷, E.J.W. Moyse⁸⁹, S. Muanza⁸⁸, R.D. Mudd¹⁹, F. Mueller¹⁰³, J. Mueller¹²⁷, R.S.P. Mueller¹⁰², D. Muenstermann⁷⁵, P. Mullen⁵⁶, G.A. Mullier¹⁸, F.J. Munoz Sanchez⁸⁷, W.J. Murray^{173,133}, H. Musheghyan⁵⁷, M. Muškinja⁷⁸, A.G. Myagkov^{132,ak}, M. Myska¹³⁰, B.P. Nachman¹⁶, O. Nackenhorst⁵², K. Nagai¹²², R. Nagai^{69,ae}, K. Nagano⁶⁹, Y. Nagasaka⁶¹, K. Nagata¹⁶⁴, M. Nagel⁵¹, E. Nagy⁸⁸, A.M. Nairz³², Y. Nakahama¹⁰⁵, K. Nakamura⁶⁹, T. Nakamura¹⁵⁷, I. Nakano¹¹⁴, R.F. Naranjo Garcia⁴⁵, R. Narayan¹¹, D.I. Narrias Villar^{60a}, I. Naryshkin¹²⁵, T. Naumann⁴⁵, G. Navarro²¹, R. Nayyar⁷, H.A. Neal⁹², P.Yu. Nechaeva⁹⁸, T.J. Neep¹³⁸, A. Negri^{123a,123b}, M. Negrini^{22a}, S. Nektarijevic¹⁰⁸, C. Nellist¹¹⁹, A. Nelson¹⁶⁶, S. Nemecek¹²⁹, P. Nemethy¹¹², A.A. Nepomuceno^{26a}, M. Nessi^{32,al}, M.S. Neubauer¹⁶⁹, M. Neumann¹⁷⁸, R.M. Neves¹¹², P. Nevski²⁷, P.R. Newman¹⁹, T.Y. Ng^{62c}, T. Nguyen Manh⁹⁷, R.B. Nickerson¹²², R. Nicolaidou¹³⁸, J. Nielsen¹³⁹, V. Nikolaenko^{132,ak}, I. Nikolic-Audit⁸³, K. Nikolopoulos¹⁹, J.K. Nilsen¹²¹, P. Nilsson²⁷, Y. Ninomiya¹⁵⁷, A. Nisati^{134a}, N. Nishu^{35c}, R. Nisius¹⁰³, T. Nobe¹⁵⁷, Y. Noguchi⁷¹, M. Nomachi¹²⁰, I. Nomidis³¹, M.A. Nomura²⁷, T. Nooney⁷⁹, M. Nordberg³², N. Norjoharuddeen¹²², O. Novgorodova⁴⁷, S. Nowak¹⁰³, M. Nozaki⁶⁹, L. Nozka¹¹⁷, K. Ntekas¹⁶⁶, E. Nurse⁸¹, F. Nuti⁹¹, D.C. O’Neil¹⁴⁴, A.A. O’Rourke⁴⁵, V. O’Shea⁵⁶, F.G. Oakham^{31,e}, H. Oberlack¹⁰³, T. Obermann²³, J. Ocariz⁸³, A. Ochi⁷⁰, I. Ochoa³⁸, J.P. Ochoa-Ricoux^{34a}, S. Oda⁷³, S. Odaka⁶⁹, H. Ogren⁶⁴, A. Oh⁸⁷, S.H. Oh⁴⁸, C.C. Ohm¹⁶, H. Ohman¹⁶⁸, H. Oide^{53a,53b}, H. Okawa¹⁶⁴, Y. Okumura¹⁵⁷, T. Okuyama⁶⁹, A. Olariu^{28b}, L.F. Oleiro Seabra^{128a}, S.A. Olivares Pino⁴⁹, D. Oliveira Damazio²⁷, A. Olszewski⁴², J. Olszowska⁴², A. Onofre^{128a,128e}, K. Onogi¹⁰⁵, P.U.E. Onyisi^{11,aa}, M.J. Oreglia³³, Y. Oren¹⁵⁵, D. Orestano^{136a,136b}, N. Orlando^{62b}, R.S. Orr¹⁶¹, B. Osculati^{53a,53b,*}, R. Ospanov⁸⁷, G. Otero y Garzon²⁹, H. Otono⁷³, M. Ouchrif^{137d}, F. Ould-Saada¹²¹, A. Ouraou¹³⁸, K.P. Oussoren¹⁰⁹, Q. Ouyang^{35a}, M. Owen⁵⁶, R.E. Owen¹⁹, V.E. Ozcan^{20a}, N. Ozturk⁸, K. Pachal¹⁴⁴, A. Pacheco Pages¹³, L. Pacheco Rodriguez¹³⁸, C. Padilla Aranda¹³, S. Pagan Griso¹⁶, M. Paganini¹⁷⁹, F. Paige²⁷, P. Pais⁸⁹, G. Palacino⁶⁴, S. Palazzo^{40a,40b}, S. Palestini³², M. Palka^{41b}, D. Pallin³⁷, E. St. Panagiotopoulou¹⁰, I. Panagoulas¹⁰, C.E. Pandini⁸³, J.G. Panduro Vazquez⁸⁰, P. Pani³², S. Panitkin²⁷, D. Pantea^{28b}, L. Paolozzi⁵², Th.D. Papadopoulou¹⁰, K. Papageorgiou⁹, A. Paramonov⁶, D. Paredes Hernandez¹⁷⁹, A.J. Parker⁷⁵, M.A. Parker³⁰, K.A. Parker⁴⁵, F. Parodi^{53a,53b}, J.A. Parsons³⁸, U. Parzefall⁵¹, V.R. Pascuzzi¹⁶¹, J.M. Pasner¹³⁹, E. Pasqualucci^{134a}, S. Passaggio^{53a}, Fr. Pastore⁸⁰, S. Patariaia¹⁷⁸, J.R. Pater⁸⁷, T. Pauly³², J. Pearce¹⁷², B. Pearson¹¹⁵, L.E. Pedersen³⁹, S. Pedraza Lopez¹⁷⁰, R. Pedro^{128a,128b}, S.V. Peleganchuk^{111,d}, O. Penc¹²⁹, C. Peng^{35a}, H. Peng^{36a}, J. Penwell⁶⁴, B.S. Peralva^{26b}, M.M. Perego¹³⁸, D.V. Perepelitsa²⁷, L. Perini^{94a,94b}, H. Pernegger³², S. Perrella^{106a,106b}, R. Peschke⁴⁵, V.D. Peshekhonov⁶⁸, K. Peters⁴⁵, R.F.Y. Peters⁸⁷, B.A. Petersen³², T.C. Petersen³⁹, E. Petit⁵⁸, A. Petridis¹, C. Petridou¹⁵⁶, P. Petroff¹¹⁹, E. Petrolo^{134a}, M. Petrov¹²², F. Petrucci^{136a,136b}, N.E. Pettersson⁸⁹, A. Peyaud¹³⁸, R. Pezoa^{34b}, P.W. Phillips¹³³, G. Piacquadio¹⁵⁰, E. Pianori¹⁷³, A. Picazio⁸⁹, E. Piccaro⁷⁹, M.A. Pickering¹²², R. Piegaia²⁹, J.E. Pilcher³³, A.D. Pilkington⁸⁷, A.W.J. Pin⁸⁷, M. Pinamonti^{167a,167c,am}, J.L. Pinfold³, H. Pirumov⁴⁵, M. Pitt¹⁷⁵, L. Plazak^{146a}, M.-A. Pleier²⁷, V. Pleskot⁸⁶, E. Plotnikova⁶⁸, D. Pluth⁶⁷, P. Podberezko¹¹¹, R. Poettgen^{148a,148b}, L. Poggioli¹¹⁹, D. Pohl²³, G. Polesello^{123a}, A. Poley⁴⁵, A. Policicchio^{40a,40b}, R. Polifka³², A. Polini^{22a}, C.S. Pollard⁵⁶, V. Polychronakos²⁷, K. Pommès³², L. Pontecorvo^{134a}, B.G. Pope⁹³, G.A. Popeneciu^{28d}, A. Poppleton³², S. Pospisil¹³⁰, K. Potamianos¹⁶, I.N. Potrap⁶⁸, C.J. Potter³⁰, C.T. Potter¹¹⁸, G. Poulard³², J. Poveda³², M.E. Pozo Astigarraga³², P. Pralavorio⁸⁸, A. Pranko¹⁶, S. Prell⁶⁷, D. Price⁸⁷, L.E. Price⁶, M. Primavera^{76a}, S. Prince⁹⁰,

K. Prokofiev^{62c}, F. Prokoshin^{34b}, S. Protopopescu²⁷, J. Proudfoot⁶, M. Przybycien^{41a}, D. Puddu^{136a,136b},
 A. Puri¹⁶⁹, P. Puzo¹¹⁹, J. Qian⁹², G. Qin⁵⁶, Y. Qin⁸⁷, A. Quadt⁵⁷, W.B. Quayle^{167a,167b},
 M. Queitsch-Maitland⁴⁵, D. Quilty⁵⁶, S. Raddum¹²¹, V. Radeka²⁷, V. Radescu¹²², S.K. Radhakrishnan¹⁵⁰,
 P. Radloff¹¹⁸, P. Rados⁹¹, F. Ragusa^{94a,94b}, G. Rahal¹⁸¹, J.A. Raine⁸⁷, S. Rajagopalan²⁷,
 C. Rangel-Smith¹⁶⁸, M.G. Ratti^{94a,94b}, D.M. Rauch⁴⁵, F. Rauscher¹⁰², S. Rave⁸⁶, T. Ravenscroft⁵⁶,
 I. Ravinovich¹⁷⁵, M. Raymond³², A.L. Read¹²¹, N.P. Readioff⁷⁷, M. Reale^{76a,76b}, D.M. Rebutzi^{123a,123b},
 A. Redelbach¹⁷⁷, G. Redlinger²⁷, R. Reece¹³⁹, R.G. Reed^{147c}, K. Reeves⁴⁴, L. Rehnisch¹⁷, J. Reichert¹²⁴,
 A. Reiss⁸⁶, C. Rembser³², H. Ren^{35a}, M. Rescigno^{134a}, S. Resconi^{94a}, E.D. Resseguie¹²⁴, S. Rettie¹⁷¹,
 E. Reynolds¹⁹, O.L. Rezanova^{111,d}, P. Reznicek¹³¹, R. Rezvani⁹⁷, R. Richter¹⁰³, S. Richter⁸¹,
 E. Richter-Was^{41b}, O. Ricken²³, M. Ridel⁸³, P. Rieck¹⁰³, C.J. Riegel¹⁷⁸, J. Rieger⁵⁷, O. Rifki¹¹⁵,
 M. Rijssenbeek¹⁵⁰, A. Rimoldi^{123a,123b}, M. Rimoldi¹⁸, L. Rinaldi^{22a}, B. Ristić⁵², E. Ritsch³², I. Riu¹³,
 F. Rizatdinova¹¹⁶, E. Rizvi⁷⁹, C. Rizzi¹³, R.T. Roberts⁸⁷, S.H. Robertson^{90,p}, A. Robichaud-Veronneau⁹⁰,
 D. Robinson³⁰, J.E.M. Robinson⁴⁵, A. Robson⁵⁶, C. Roda^{126a,126b}, Y. Rodina^{88,an}, A. Rodriguez Perez¹³,
 D. Rodriguez Rodriguez¹⁷⁰, S. Roe³², C.S. Rogan⁵⁹, O. Röhne¹²¹, J. Roloff⁵⁹, A. Romaniouk¹⁰⁰,
 M. Romano^{22a,22b}, S.M. Romano Saez³⁷, E. Romero Adam¹⁷⁰, N. Rompotis⁷⁷, M. Ronzani⁵¹, L. Roos⁸³,
 S. Rosati^{134a}, K. Rosbach⁵¹, P. Rose¹³⁹, N.-A. Rosien⁵⁷, V. Rossetti^{148a,148b}, E. Rossi^{106a,106b},
 L.P. Rossi^{53a}, J.H.N. Rosten³⁰, R. Rosten¹⁴⁰, M. Rotaru^{28b}, I. Roth¹⁷⁵, J. Rothberg¹⁴⁰, D. Rousseau¹¹⁹,
 A. Rozanov⁸⁸, Y. Rozen¹⁵⁴, X. Ruan^{147c}, F. Rubbo¹⁴⁵, F. Rühr⁵¹, A. Ruiz-Martinez³¹, Z. Rurikova⁵¹,
 N.A. Rusakovich⁶⁸, A. Ruschke¹⁰², H.L. Russell¹⁴⁰, J.P. Rutherford⁷, N. Ruthmann³², Y.F. Ryabov¹²⁵,
 M. Rybar¹⁶⁹, G. Rybkin¹¹⁹, S. Ryu⁶, A. Ryzhov¹³², G.F. Rzehorz⁵⁷, A.F. Saavedra¹⁵², G. Sabato¹⁰⁹,
 S. Sacerdoti²⁹, H.F.-W. Sadrozinski¹³⁹, R. Sadykov⁶⁸, F. Safai Tehrani^{134a}, P. Saha¹¹⁰, M. Sahinsoy^{60a},
 M. Saimpert⁴⁵, T. Saito¹⁵⁷, H. Sakamoto¹⁵⁷, Y. Sakurai¹⁷⁴, G. Salamanna^{136a,136b}, J.E. Salazar Loyola^{34b},
 D. Salek¹⁰⁹, P.H. Sales De Bruin¹⁴⁰, D. Salihagic¹⁰³, A. Salmikov¹⁴⁵, J. Salt¹⁷⁰, D. Salvatore^{40a,40b},
 F. Salvatore¹⁵¹, A. Salvucci^{62a,62b,62c}, A. Salzburger³², D. Sammel⁵¹, D. Sampsonidis¹⁵⁶, J. Sánchez¹⁷⁰,
 V. Sanchez Martinez¹⁷⁰, A. Sanchez Pineda^{106a,106b}, H. Sandaker¹²¹, R.L. Sandbach⁷⁹, C.O. Sander⁴⁵,
 M. Sandhoff¹⁷⁸, C. Sandoval²¹, D.P.C. Sankey¹³³, M. Sannino^{53a,53b}, A. Sansoni⁵⁰, C. Santoni³⁷,
 R. Santonico^{135a,135b}, H. Santos^{128a}, I. Santoyo Castillo¹⁵¹, K. Sapp¹²⁷, A. Saponov⁶⁸,
 J.G. Saraiva^{128a,128d}, B. Sarrazin²³, O. Sasaki⁶⁹, K. Sato¹⁶⁴, E. Sauvan⁵, G. Savage⁸⁰, P. Savard^{161,e},
 N. Savic¹⁰³, C. Sawyer¹³³, L. Sawyer^{82,v}, J. Saxon³³, C. Sbarra^{22a}, A. Sbrizzi^{22a,22b}, T. Scanlon⁸¹,
 D.A. Scannicchio¹⁶⁶, M. Scarcella¹⁵², V. Scarfone^{40a,40b}, J. Schaarschmidt¹⁴⁰, P. Schacht¹⁰³,
 B.M. Schachtner¹⁰², D. Schaefer³², L. Schaefer¹²⁴, R. Schaefer⁴⁵, J. Schaeffer⁸⁶, S. Schaepe²³,
 S. Schaezel^{60b}, U. Schäfer⁸⁶, A.C. Schaffer¹¹⁹, D. Schaile¹⁰², R.D. Schamberger¹⁵⁰, V. Scharf^{60a},
 V.A. Schegelsky¹²⁵, D. Scheirich¹³¹, M. Schernau¹⁶⁶, C. Schiavi^{53a,53b}, S. Schier¹³⁹, C. Schillo⁵¹,
 M. Schioppa^{40a,40b}, S. Schlenker³², K.R. Schmidt-Sommerfeld¹⁰³, K. Schmieden³², C. Schmitt⁸⁶,
 S. Schmitt⁴⁵, S. Schmitz⁸⁶, B. Schneider^{163a}, U. Schnoor⁵¹, L. Schoeffel¹³⁸, A. Schoening^{60b},
 B.D. Schoenrock⁹³, E. Schopf²³, M. Schott⁸⁶, J.F.P. Schouwenberg¹⁰⁸, J. Schovancova⁸, S. Schramm⁵²,
 N. Schuh⁸⁶, A. Schulte⁸⁶, M.J. Schultens²³, H.-C. Schultz-Coulon^{60a}, H. Schulz¹⁷, M. Schumacher⁵¹,
 B.A. Schumm¹³⁹, Ph. Schune¹³⁸, A. Schwartzman¹⁴⁵, T.A. Schwarz⁹², H. Schweiger⁸⁷,
 Ph. Schwemling¹³⁸, R. Schwienhorst⁹³, J. Schwindling¹³⁸, T. Schwindt²³, G. Sciolla²⁵, F. Scuri^{126a,126b},
 F. Scutti⁹¹, J. Searcy⁹², P. Seema²³, S.C. Seidel¹⁰⁷, A. Seiden¹³⁹, J.M. Seixas^{26a}, G. Sekhniaidze^{106a},
 K. Sekhon⁹², S.J. Sekula⁴³, N. Semprini-Cesari^{22a,22b}, C. Serfon¹²¹, L. Serin¹¹⁹, L. Serkin^{167a,167b},
 M. Sessa^{136a,136b}, R. Seuster¹⁷², H. Severini¹¹⁵, T. Sfiligoi⁷⁸, F. Sforza³², A. Sfyrla⁵², E. Shabalina⁵⁷,
 N.W. Shaikh^{148a,148b}, L.Y. Shan^{35a}, R. Shang¹⁶⁹, J.T. Shank²⁴, M. Shapiro¹⁶, P.B. Shatalov⁹⁹,
 K. Shaw^{167a,167b}, S.M. Shaw⁸⁷, A. Shcherbakova^{148a,148b}, C.Y. Shehu¹⁵¹, Y. Shen¹¹⁵, P. Sherwood⁸¹,
 L. Shi^{153,ao}, S. Shimizu⁷⁰, C.O. Shimmin¹⁷⁹, M. Shimojima¹⁰⁴, S. Shirabe⁷³, M. Shiyakova^{68,ap},
 J. Shlomi¹⁷⁵, A. Shmeleva⁹⁸, D. Shoaleh Saadi⁹⁷, M.J. Shochet³³, S. Shojaii^{94a}, D.R. Shope¹¹⁵,
 S. Shrestha¹¹³, E. Shulga¹⁰⁰, M.A. Shupe⁷, P. Sicho¹²⁹, A.M. Sickles¹⁶⁹, P.E. Sidebo¹⁴⁹,
 E. Sideras Haddad^{147c}, O. Sidiropoulou¹⁷⁷, D. Sidorov¹¹⁶, A. Sidoti^{22a,22b}, F. Siegert⁴⁷, Dj. Sijacki¹⁴,
 J. Silva^{128a,128d}, S.B. Silverstein^{148a}, V. Simak¹³⁰, Lj. Simic¹⁴, S. Simion¹¹⁹, E. Simioni⁸⁶, B. Simmons⁸¹,
 M. Simon⁸⁶, P. Sinervo¹⁶¹, N.B. Sinev¹¹⁸, M. Sioli^{22a,22b}, G. Siragusa¹⁷⁷, I. Siral⁹², S.Yu. Sivoklokov¹⁰¹,
 J. Sjölin^{148a,148b}, M.B. Skinner⁷⁵, P. Skubic¹¹⁵, M. Slater¹⁹, T. Slavicek¹³⁰, M. Slawinska¹⁰⁹, K. Sliwa¹⁶⁵,
 R. Slovak¹³¹, V. Smakhtin¹⁷⁵, B.H. Smart⁵, L. Smestad¹⁵, J. Smiesko^{146a}, S.Yu. Smirnov¹⁰⁰,

Y. Smirnov¹⁰⁰, L.N. Smirnova^{101,aq}, O. Smirnova⁸⁴, J.W. Smith⁵⁷, M.N.K. Smith³⁸, R.W. Smith³⁸,
 M. Smizanska⁷⁵, K. Smolek¹³⁰, A.A. Snesarev⁹⁸, I.M. Snyder¹¹⁸, S. Snyder²⁷, R. Sobie^{172,p}, F. Socher⁴⁷,
 A. Soffer¹⁵⁵, D.A. Soh¹⁵³, G. Sokhrannyi⁷⁸, C.A. Solans Sanchez³², M. Solar¹³⁰, E.Yu. Soldatov¹⁰⁰,
 U. Soldevila¹⁷⁰, A.A. Solodkov¹³², A. Soloshenko⁶⁸, O.V. Solovyanov¹³², V. Solovyev¹²⁵, P. Sommer⁵¹,
 H. Son¹⁶⁵, H.Y. Song^{36a,ar}, A. Sopczak¹³⁰, V. Sorin¹³, D. Sosa^{60b}, C.L. Sotiropoulou^{126a,126b},
 R. Soualah^{167a,167c}, A.M. Soukharev^{111,d}, D. South⁴⁵, B.C. Sowden⁸⁰, S. Spagnolo^{76a,76b},
 M. Spalla^{126a,126b}, M. Spangenberg¹⁷³, F. Spanò⁸⁰, D. Sperlich¹⁷, F. Spettel¹⁰³, T.M. Spieker^{60a},
 R. Spighi^{22a}, G. Spigo³², L.A. Spiller⁹¹, M. Spousta¹³¹, R.D. St. Denis^{56,*}, A. Stabile^{94a}, R. Stamen^{60a},
 S. Stamm¹⁷, E. Stanecka⁴², R.W. Stanek⁶, C. Stanescu^{136a}, M.M. Stanitzki⁴⁵, S. Stapnes¹²¹,
 E.A. Starchenko¹³², G.H. Stark³³, J. Stark⁵⁸, S.H. Stark³⁹, P. Staroba¹²⁹, P. Starovoitov^{60a}, S. Stärz³²,
 R. Staszewski⁴², P. Steinberg²⁷, B. Stelzer¹⁴⁴, H.J. Stelzer³², O. Stelzer-Chilton^{163a}, H. Stenzel⁵⁵,
 G.A. Stewart⁵⁶, J.A. Stillings²³, M.C. Stockton⁹⁰, M. Stoebe⁹⁰, G. Stoicea^{28b}, P. Stolte⁵⁷, S. Stonjek¹⁰³,
 A.R. Stradling⁸, A. Straessner⁴⁷, M.E. Stramaglia¹⁸, J. Strandberg¹⁴⁹, S. Strandberg^{148a,148b},
 A. Strandlie¹²¹, M. Strauss¹¹⁵, P. Strizenec^{146b}, R. Ströhmer¹⁷⁷, D.M. Strom¹¹⁸, R. Stroynowski⁴³,
 A. Strubig¹⁰⁸, S.A. Stucci²⁷, B. Stugu¹⁵, N.A. Styles⁴⁵, D. Su¹⁴⁵, J. Su¹²⁷, S. Suchek^{60a}, Y. Sugaya¹²⁰,
 M. Suk¹³⁰, V.V. Sulim⁹⁸, S. Sultansoy^{4c}, T. Sumida⁷¹, S. Sun⁵⁹, X. Sun³, K. Suruliz¹⁵¹, C.J.E. Suster¹⁵²,
 M.R. Sutton¹⁵¹, S. Suzuki⁶⁹, M. Svatos¹²⁹, M. Swiatkowski³³, S.P. Swift², I. Sykora^{146a}, T. Sykora¹³¹,
 D. Ta⁵¹, K. Tackmann⁴⁵, J. Taenzer¹⁵⁵, A. Taffard¹⁶⁶, R. Tafirout^{163a}, N. Taiblum¹⁵⁵, H. Takai²⁷,
 R. Takashima⁷², T. Takeshita¹⁴², Y. Takubo⁶⁹, M. Talby⁸⁸, A.A. Talyshiev^{111,d}, J. Tanaka¹⁵⁷, M. Tanaka¹⁵⁹,
 R. Tanaka¹¹⁹, S. Tanaka⁶⁹, R. Tanioka⁷⁰, B.B. Tannenwald¹¹³, S. Tapia Araya^{34b}, S. Tapprogge⁸⁶,
 S. Tarem¹⁵⁴, G.F. Tartarelli^{94a}, P. Tas¹³¹, M. Tasevsky¹²⁹, T. Tashiro⁷¹, E. Tassi^{40a,40b},
 A. Tavares Delgado^{128a,128b}, Y. Tayalati^{137e}, A.C. Taylor¹⁰⁷, G.N. Taylor⁹¹, P.T.E. Taylor⁹¹, W. Taylor^{163b},
 P. Teixeira-Dias⁸⁰, D. Temple¹⁴⁴, H. Ten Kate³², P.K. Teng¹⁵³, J.J. Teoh¹²⁰, F. Tepel¹⁷⁸, S. Terada⁶⁹,
 K. Terashi¹⁵⁷, J. Terron⁸⁵, S. Terzo¹³, M. Testa⁵⁰, R.J. Teuscher^{161,p}, T. Theveneaux-Pelzer⁸⁸,
 J.P. Thomas¹⁹, J. Thomas-Wilsker⁸⁰, P.D. Thompson¹⁹, A.S. Thompson⁵⁶, L.A. Thomsen¹⁷⁹,
 E. Thomson¹²⁴, M.J. Tibbetts¹⁶, R.E. Ticse Torres⁸⁸, V.O. Tikhomirov^{98,as}, Yu.A. Tikhonov^{111,d},
 S. Timoshenko¹⁰⁰, P. Tipton¹⁷⁹, S. Tisserant⁸⁸, K. Todome¹⁵⁹, S. Todorova-Nova⁵, J. Tojo⁷³, S. Tokár^{146a},
 K. Tokushuku⁶⁹, E. Tolley⁵⁹, L. Tomlinson⁸⁷, M. Tomoto¹⁰⁵, L. Tompkins^{145,at}, K. Toms¹⁰⁷, B. Tong⁵⁹,
 P. Tornambe⁵¹, E. Torrence¹¹⁸, H. Torres¹⁴⁴, E. Torrón Pastor¹⁴⁰, J. Toth^{88,au}, F. Touchard⁸⁸,
 D.R. Tovey¹⁴¹, C.J. Treado¹¹², T. Trefzger¹⁷⁷, A. Tricoli²⁷, I.M. Trigger^{163a}, S. Trincaz-Duvoid⁸³,
 M.F. Tripiana¹³, W. Trischuk¹⁶¹, B. Trocmé⁵⁸, A. Trofymov⁴⁵, C. Troncon^{94a}, M. Trottier-McDonald¹⁶,
 M. Trovatelli¹⁷², L. Truong^{167a,167c}, M. Trzebinski⁴², A. Trzupek⁴², K.W. Tsang^{62a}, J.C.-L. Tseng¹²²,
 P.V. Tsiarehshka⁹⁵, G. Tsipolitis¹⁰, N. Tsirintanis⁹, S. Tsiskaridze¹³, V. Tsiskaridze⁵¹, E.G. Tskhadadze^{54a},
 K.M. Tsui^{62a}, I.I. Tsukerman⁹⁹, V. Tsulaia¹⁶, S. Tsuno⁶⁹, D. Tsybychev¹⁵⁰, Y. Tu^{62b}, A. Tudorache^{28b},
 V. Tudorache^{28b}, T.T. Tulbure^{28a}, A.N. Tuna⁵⁹, S.A. Tupputi^{22a,22b}, S. Turchikhin⁶⁸, D. Turgeman¹⁷⁵,
 I. Turk Cakir^{4b,av}, R. Turra^{94a,94b}, P.M. Tuts³⁸, G. Ucchielli^{22a,22b}, I. Ueda⁶⁹, M. Ughetto^{148a,148b},
 F. Ukegawa¹⁶⁴, G. Unal³², A. Undrus²⁷, G. Unel¹⁶⁶, F.C. Ungaro⁹¹, Y. Unno⁶⁹, C. Unverdorben¹⁰²,
 J. Urban^{146b}, P. Urquijo⁹¹, P. Urrejola⁸⁶, G. Usai⁸, J. Usui⁶⁹, L. Vacavant⁸⁸, V. Vacek¹³⁰, B. Vachon⁹⁰,
 C. Valderanis¹⁰², E. Valdes Santurio^{148a,148b}, N. Valencic¹⁰⁹, S. Valentini^{22a,22b}, A. Valero¹⁷⁰,
 L. Valéry¹³, S. Valkar¹³¹, A. Vallier⁵, J.A. Valls Ferrer¹⁷⁰, W. Van Den Wollenberg¹⁰⁹,
 H. van der Graaf¹⁰⁹, N. van Eldik¹⁵⁴, P. van Gemmeren⁶, J. Van Nieuwkoop¹⁴⁴, I. van Vulpen¹⁰⁹,
 M.C. van Woerden¹⁰⁹, M. Vanadia^{134a,134b}, W. Vandelli³², R. Vanguri¹²⁴, A. Vaniachine¹⁶⁰,
 P. Vankov¹⁰⁹, G. Vardanyan¹⁸⁰, R. Vari^{134a}, E.W. Varnes⁷, C. Varni^{53a,53b}, T. Varol⁴³, D. Varouchas⁸³,
 A. Vartapetian⁸, K.E. Varvell¹⁵², J.G. Vasquez¹⁷⁹, G.A. Vasquez^{34b}, F. Vazeille³⁷, T. Vazquez Schroeder⁹⁰,
 J. Veatch⁵⁷, V. Veeraraghavan⁷, L.M. Veloce¹⁶¹, F. Veloso^{128a,128c}, S. Veneziano^{134a}, A. Ventura^{76a,76b},
 M. Venturi¹⁷², N. Venturi¹⁶¹, A. Venturini²⁵, V. Vercesi^{123a}, M. Verducci^{136a,136b}, W. Verkerke¹⁰⁹,
 J.C. Vermeulen¹⁰⁹, M.C. Vetterli^{144,e}, N. Viaux Maira^{34a}, O. Viazlo⁸⁴, I. Vichou^{169,*}, T. Vickey¹⁴¹,
 O.E. Vickey Boeriu¹⁴¹, G.H.A. Viehhauser¹²², S. Viel¹⁶, L. Vigani¹²², M. Villa^{22a,22b},
 M. Villaplana Perez^{94a,94b}, E. Vilucchi⁵⁰, M.G. Vincker³¹, V.B. Vinogradov⁶⁸, A. Vishwakarma⁴⁵,
 C. Vittori^{22a,22b}, I. Vivarelli¹⁵¹, S. Vlachos¹⁰, M. Vlasak¹³⁰, M. Vogel¹⁷⁸, P. Vokac¹³⁰, G. Volpi^{126a,126b},
 M. Volpi⁹¹, H. von der Schmitt¹⁰³, E. von Toerne²³, V. Vorobel¹³¹, K. Vorobev¹⁰⁰, M. Vos¹⁷⁰, R. Voss³²,
 J.H. Vossebeld⁷⁷, N. Vranjes¹⁴, M. Vranjes Milosavljevic¹⁴, V. Vrba¹³⁰, M. Vreeswijk¹⁰⁹, R. Vuillermet³²,

I. Vukotic³³, P. Wagner²³, W. Wagner¹⁷⁸, H. Wahlberg⁷⁴, S. Wahrmund⁴⁷, J. Wakabayashi¹⁰⁵, J. Walder⁷⁵, R. Walker¹⁰², W. Walkowiak¹⁴³, V. Wallangen^{148a,148b}, C. Wang^{35b}, C. Wang^{36b,aw}, F. Wang¹⁷⁶, H. Wang¹⁶, H. Wang³, J. Wang⁴⁵, J. Wang¹⁵², Q. Wang¹¹⁵, R. Wang⁶, S.M. Wang¹⁵³, T. Wang³⁸, W. Wang^{153,ax}, W. Wang^{36a}, C. Wanotayaroj¹¹⁸, A. Warburton⁹⁰, C.P. Ward³⁰, D.R. Wardrope⁸¹, A. Washbrook⁴⁹, P.M. Watkins¹⁹, A.T. Watson¹⁹, M.F. Watson¹⁹, G. Watts¹⁴⁰, S. Watts⁸⁷, B.M. Waugh⁸¹, A.F. Webb¹¹, S. Webb⁸⁶, M.S. Weber¹⁸, S.W. Weber¹⁷⁷, S.A. Weber³¹, J.S. Webster⁶, A.R. Weidberg¹²², B. Weinert⁶⁴, J. Weingarten⁵⁷, C. Weiser⁵¹, H. Weits¹⁰⁹, P.S. Wells³², T. Wenaus²⁷, T. Wengler³², S. Wenig³², N. Wermes²³, M.D. Werner⁶⁷, P. Werner³², M. Wessels^{60a}, K. Whalen¹¹⁸, N.L. Whallon¹⁴⁰, A.M. Wharton⁷⁵, A. White⁸, M.J. White¹, R. White^{34b}, D. Whiteson¹⁶⁶, F.J. Wickens¹³³, W. Wiedenmann¹⁷⁶, M. Wielers¹³³, C. Wiglesworth³⁹, L.A.M. Wiik-Fuchs²³, A. Wildauer¹⁰³, F. Wilk⁸⁷, H.G. Wilkens³², H.H. Williams¹²⁴, S. Williams¹⁰⁹, C. Willis⁹³, S. Willocq⁸⁹, J.A. Wilson¹⁹, I. Wingerter-Seez⁵, F. Winklmeier¹¹⁸, O.J. Winston¹⁵¹, B.T. Winter²³, M. Wittgen¹⁴⁵, M. Wobisch^{82,v}, T.M.H. Wolf¹⁰⁹, R. Wolff⁸⁸, M.W. Wolter⁴², H. Wolters^{128a,128c}, S.D. Worm¹⁹, B.K. Wosiek⁴², J. Wotschack³², M.J. Woudstra⁸⁷, K.W. Wozniak⁴², M. Wu³³, S.L. Wu¹⁷⁶, X. Wu⁵², Y. Wu⁹², T.R. Wyatt⁸⁷, B.M. Wynne⁴⁹, S. Xella³⁹, Z. Xi⁹², L. Xia^{35c}, D. Xu^{35a}, L. Xu²⁷, B. Yabsley¹⁵², S. Yacoob^{147a}, D. Yamaguchi¹⁵⁹, Y. Yamaguchi¹²⁰, A. Yamamoto⁶⁹, S. Yamamoto¹⁵⁷, T. Yamanaka¹⁵⁷, K. Yamauchi¹⁰⁵, Y. Yamazaki⁷⁰, Z. Yan²⁴, H. Yang^{36c}, H. Yang¹⁶, Y. Yang¹⁵³, Z. Yang¹⁵, W-M. Yao¹⁶, Y.C. Yap⁸³, Y. Yasu⁶⁹, E. Yatsenko⁵, K.H. Yau Wong²³, J. Ye⁴³, S. Ye²⁷, I. Yeletsikh⁶⁸, E. Yildirim⁸⁶, K. Yorita¹⁷⁴, K. Yoshihara¹²⁴, C. Young¹⁴⁵, C.J.S. Young³², S. Youssef²⁴, D.R. Yu¹⁶, J. Yu⁸, J. Yu⁶⁷, L. Yuan⁷⁰, S.P.Y. Yuen²³, I. Yusuff^{30,ay}, B. Zabinski⁴², G. Zacharis¹⁰, R. Zaidan¹³, A.M. Zaitsev^{132,ak}, N. Zakharchuk⁴⁵, J. Zalieckas¹⁵, A. Zaman¹⁵⁰, S. Zambito⁵⁹, D. Zanzi⁹¹, C. Zeitnitz¹⁷⁸, M. Zeman¹³⁰, A. Zemla^{41a}, J.C. Zeng¹⁶⁹, Q. Zeng¹⁴⁵, O. Zenin¹³², T. Ženiš^{146a}, D. Zerwas¹¹⁹, D. Zhang⁹², F. Zhang¹⁷⁶, G. Zhang^{36a,ar}, H. Zhang^{35b}, J. Zhang⁶, L. Zhang⁵¹, L. Zhang^{36a}, M. Zhang¹⁶⁹, R. Zhang²³, R. Zhang^{36a,aw}, X. Zhang^{36b}, Y. Zhang^{35a}, Z. Zhang¹¹⁹, X. Zhao⁴³, Y. Zhao^{36b,az}, Z. Zhao^{36a}, A. Zhemchugov⁶⁸, J. Zhong¹²², B. Zhou⁹², C. Zhou¹⁷⁶, L. Zhou⁴³, M. Zhou^{35a}, M. Zhou¹⁵⁰, N. Zhou^{35c}, C.G. Zhu^{36b}, H. Zhu^{35a}, J. Zhu⁹², Y. Zhu^{36a}, X. Zhuang^{35a}, K. Zhukov⁹⁸, A. Zibell¹⁷⁷, D. Zieminska⁶⁴, N.I. Zimine⁶⁸, C. Zimmermann⁸⁶, S. Zimmermann⁵¹, Z. Zinonos¹⁰³, M. Zinser⁸⁶, M. Ziolkowski¹⁴³, L. Živković¹⁴, G. Zobernig¹⁷⁶, A. Zoccoli^{22a,22b}, R. Zou³³, M. zur Nedden¹⁷, L. Zwalinski³²

¹ Department of Physics, University of Adelaide, Adelaide, Australia

² Physics Department, SUNY Albany, Albany NY, United States

³ Department of Physics, University of Alberta, Edmonton AB, Canada

⁴ (a) Department of Physics, Ankara University, Ankara; (b) Istanbul Aydin University, Istanbul; (c) Division of Physics, TOBB Istanbul University of Economics and Technology, Ankara, Turkey

⁵ LAPP, CNRS/IN2P3 and Université Savoie Mont Blanc, Annecy-le-Vieux, France

⁶ High Energy Physics Division, Argonne National Laboratory, Argonne IL, United States

⁷ Department of Physics, University of Arizona, Tucson AZ, United States

⁸ Department of Physics, The University of Texas at Arlington, Arlington TX, United States

⁹ Physics Department, National and Kapodistrian University of Athens, Athens, Greece

¹⁰ Physics Department, National Technical University of Athens, Zografou, Greece

¹¹ Department of Physics, The University of Texas at Austin, Austin TX, United States

¹² Institute of Physics, Azerbaijan Academy of Sciences, Baku, Azerbaijan

¹³ Institut de Física d'Altes Energies (IFAE), The Barcelona Institute of Science and Technology, Barcelona, Spain

¹⁴ Institute of Physics, University of Belgrade, Belgrade, Serbia

¹⁵ Department for Physics and Technology, University of Bergen, Bergen, Norway

¹⁶ Physics Division, Lawrence Berkeley National Laboratory and University of California, Berkeley CA, United States

¹⁷ Department of Physics, Humboldt University, Berlin, Germany

¹⁸ Albert Einstein Center for Fundamental Physics and Laboratory for High Energy Physics, University of Bern, Bern, Switzerland

¹⁹ School of Physics and Astronomy, University of Birmingham, Birmingham, United Kingdom

²⁰ (a) Department of Physics, Bogazici University, Istanbul; (b) Department of Physics Engineering, Gaziantep University, Gaziantep; (d) Istanbul Bilgi University, Faculty of Engineering and Natural Sciences, Istanbul; (e) Bahcesehir University, Faculty of Engineering and Natural Sciences, Istanbul, Turkey

²¹ Centro de Investigaciones, Universidad Antonio Narino, Bogota, Colombia

²² (a) INFN Sezione di Bologna; (b) Dipartimento di Fisica e Astronomia, Università di Bologna, Bologna, Italy

²³ Physikalisches Institut, University of Bonn, Bonn, Germany

²⁴ Department of Physics, Boston University, Boston MA, United States

²⁵ Department of Physics, Brandeis University, Waltham MA, United States

²⁶ (a) Universidade Federal do Rio De Janeiro COPPE/EE/IF, Rio de Janeiro; (b) Electrical Circuits Department, Federal University of Juiz de Fora (UFJF), Juiz de Fora; (c) Federal University of Sao Joao del Rei (UFSJ), Sao Joao del Rei; (d) Instituto de Física, Universidade de Sao Paulo, Sao Paulo, Brazil

²⁷ Physics Department, Brookhaven National Laboratory, Upton NY, United States

²⁸ (a) Transilvania University of Brasov, Brasov, Romania; (b) Horia Hulubei National Institute of Physics and Nuclear Engineering, Bucharest; (c) Department of Physics, Alexandru Ioan Cuza University of Iasi, Iasi, Romania; (d) National Institute for Research and Development of Isotopic and Molecular Technologies, Physics Department, Cluj Napoca; (e) University Politehnica Bucharest, Bucharest; (f) West University in Timisoara, Timisoara, Romania

²⁹ Departamento de Física, Universidad de Buenos Aires, Buenos Aires, Argentina

³⁰ Cavendish Laboratory, University of Cambridge, Cambridge, United Kingdom

³¹ Department of Physics, Carleton University, Ottawa ON, Canada

³² CERN, Geneva, Switzerland

- ³³ Enrico Fermi Institute, University of Chicago, Chicago IL, United States
- ³⁴ ^(a) Departamento de Física, Pontificia Universidad Católica de Chile, Santiago; ^(b) Departamento de Física, Universidad Técnica Federico Santa María, Valparaíso, Chile
- ³⁵ ^(a) Institute of High Energy Physics, Chinese Academy of Sciences, Beijing; ^(b) Department of Physics, Nanjing University, Jiangsu; ^(c) Physics Department, Tsinghua University, Beijing 100084, China
- ³⁶ ^(a) Department of Modern Physics, University of Science and Technology of China, Anhui; ^(b) School of Physics, Shandong University, Shandong; ^(c) Department of Physics and Astronomy, Key Laboratory for Particle Physics, Astrophysics and Cosmology, Ministry of Education; ^(d) Shanghai Key Laboratory for Particle Physics and Cosmology, Shanghai Jiao Tong University, Shanghai, China^a
- ³⁷ Université Clermont Auvergne, CNRS/IN2P3, LPC, Clermont-Ferrand, France
- ³⁸ Nevis Laboratory, Columbia University, Irvington NY, United States
- ³⁹ Niels Bohr Institute, University of Copenhagen, Kobenhavn, Denmark
- ⁴⁰ ^(a) INFN Gruppo Collegato di Cosenza, Laboratori Nazionali di Frascati; ^(b) Dipartimento di Fisica, Università della Calabria, Rende, Italy
- ⁴¹ ^(a) AGH University of Science and Technology, Faculty of Physics and Applied Computer Science, Krakow; ^(b) Marian Smoluchowski Institute of Physics, Jagiellonian University, Krakow, Poland
- ⁴² Institute of Nuclear Physics Polish Academy of Sciences, Krakow, Poland
- ⁴³ Physics Department, Southern Methodist University, Dallas TX, United States
- ⁴⁴ Physics Department, University of Texas at Dallas, Richardson TX, United States
- ⁴⁵ DESY, Hamburg and Zeuthen, Germany
- ⁴⁶ Lehrstuhl für Experimentelle Physik IV, Technische Universität Dortmund, Dortmund, Germany
- ⁴⁷ Institut für Kern- und Teilchenphysik, Technische Universität Dresden, Dresden, Germany
- ⁴⁸ Department of Physics, Duke University, Durham NC, United States
- ⁴⁹ SUPA – School of Physics and Astronomy, University of Edinburgh, Edinburgh, United Kingdom
- ⁵⁰ INFN Laboratori Nazionali di Frascati, Frascati, Italy
- ⁵¹ Fakultät für Mathematik und Physik, Albert-Ludwigs-Universität, Freiburg, Germany
- ⁵² Département de Physique Nucléaire et Corpusculaire, Université de Genève, Geneva, Switzerland
- ⁵³ ^(a) INFN Sezione di Genova; ^(b) Dipartimento di Fisica, Università di Genova, Genova, Italy
- ⁵⁴ ^(a) E. Andronikashvili Institute of Physics, Iv. Javakishvili Tbilisi State University, Tbilisi; ^(b) High Energy Physics Institute, Tbilisi State University, Tbilisi, Georgia
- ⁵⁵ II Physikalisches Institut, Justus-Liebig-Universität Giessen, Giessen, Germany
- ⁵⁶ SUPA – School of Physics and Astronomy, University of Glasgow, Glasgow, United Kingdom
- ⁵⁷ II Physikalisches Institut, Georg-August-Universität, Göttingen, Germany
- ⁵⁸ Laboratoire de Physique Subatomique et de Cosmologie, Université Grenoble-Alpes, CNRS/IN2P3, Grenoble, France
- ⁵⁹ Laboratory for Particle Physics and Cosmology, Harvard University, Cambridge MA, United States
- ⁶⁰ ^(a) Kirchhoff-Institut für Physik, Ruprecht-Karls-Universität Heidelberg, Heidelberg; ^(b) Physikalisches Institut, Ruprecht-Karls-Universität Heidelberg, Mannheim, Germany
- ⁶¹ Faculty of Applied Information Science, Hiroshima Institute of Technology, Hiroshima, Japan
- ⁶² ^(a) Department of Physics, The Chinese University of Hong Kong, Shatin, N.T., Hong Kong; ^(b) Department of Physics, The University of Hong Kong, Hong Kong; ^(c) Department of Physics and Institute for Advanced Study, The Hong Kong University of Science and Technology, Clear Water Bay, Kowloon, Hong Kong, China
- ⁶³ Department of Physics, National Tsing Hua University, Taiwan, Taiwan
- ⁶⁴ Department of Physics, Indiana University, Bloomington IN, United States
- ⁶⁵ Institut für Astro- und Teilchenphysik, Leopold-Franzens-Universität, Innsbruck, Austria
- ⁶⁶ University of Iowa, Iowa City IA, United States
- ⁶⁷ Department of Physics and Astronomy, Iowa State University, Ames IA, United States
- ⁶⁸ Joint Institute for Nuclear Research, JINR Dubna, Dubna, Russia
- ⁶⁹ KEK, High Energy Accelerator Research Organization, Tsukuba, Japan
- ⁷⁰ Graduate School of Science, Kobe University, Kobe, Japan
- ⁷¹ Faculty of Science, Kyoto University, Kyoto, Japan
- ⁷² Kyoto University of Education, Kyoto, Japan
- ⁷³ Department of Physics, Kyushu University, Fukuoka, Japan
- ⁷⁴ Instituto de Física La Plata, Universidad Nacional de La Plata and CONICET, La Plata, Argentina
- ⁷⁵ Physics Department, Lancaster University, Lancaster, United Kingdom
- ⁷⁶ ^(a) INFN Sezione di Lecce; ^(b) Dipartimento di Matematica e Fisica, Università del Salento, Lecce, Italy
- ⁷⁷ Oliver Lodge Laboratory, University of Liverpool, Liverpool, United Kingdom
- ⁷⁸ Department of Experimental Particle Physics, Jožef Stefan Institute and Department of Physics, University of Ljubljana, Ljubljana, Slovenia
- ⁷⁹ School of Physics and Astronomy, Queen Mary University of London, London, United Kingdom
- ⁸⁰ Department of Physics, Royal Holloway University of London, Surrey, United Kingdom
- ⁸¹ Department of Physics and Astronomy, University College London, London, United Kingdom
- ⁸² Louisiana Tech University, Ruston LA, United States
- ⁸³ Laboratoire de Physique Nucléaire et de Hautes Energies, UPMC and Université Paris-Diderot and CNRS/IN2P3, Paris, France
- ⁸⁴ Fysiska institutionen, Lunds universitet, Lund, Sweden
- ⁸⁵ Departamento de Física Teórica C-15, Universidad Autónoma de Madrid, Madrid, Spain
- ⁸⁶ Institut für Physik, Universität Mainz, Mainz, Germany
- ⁸⁷ School of Physics and Astronomy, University of Manchester, Manchester, United Kingdom
- ⁸⁸ CPPM, Aix-Marseille Université and CNRS/IN2P3, Marseille, France
- ⁸⁹ Department of Physics, University of Massachusetts, Amherst MA, United States
- ⁹⁰ Department of Physics, McGill University, Montreal QC, Canada
- ⁹¹ School of Physics, University of Melbourne, Victoria, Australia
- ⁹² Department of Physics, The University of Michigan, Ann Arbor MI, United States
- ⁹³ Department of Physics and Astronomy, Michigan State University, East Lansing MI, United States
- ⁹⁴ ^(a) INFN Sezione di Milano; ^(b) Dipartimento di Fisica, Università di Milano, Milano, Italy
- ⁹⁵ B.I. Stepanov Institute of Physics, National Academy of Sciences of Belarus, Minsk, Belarus
- ⁹⁶ Research Institute for Nuclear Problems of Byelorussian State University, Minsk, Belarus
- ⁹⁷ Group of Particle Physics, University of Montreal, Montreal QC, Canada
- ⁹⁸ P.N. Lebedev Physical Institute of the Russian Academy of Sciences, Moscow, Russia
- ⁹⁹ Institute for Theoretical and Experimental Physics (ITEP), Moscow, Russia
- ¹⁰⁰ National Research Nuclear University MEPhI, Moscow, Russia
- ¹⁰¹ D.V. Skobeltsyn Institute of Nuclear Physics, M.V. Lomonosov Moscow State University, Moscow, Russia
- ¹⁰² Fakultät für Physik, Ludwig-Maximilians-Universität München, München, Germany
- ¹⁰³ Max-Planck-Institut für Physik (Werner-Heisenberg-Institut), München, Germany
- ¹⁰⁴ Nagasaki Institute of Applied Science, Nagasaki, Japan
- ¹⁰⁵ Graduate School of Science and Kobayashi-Maskawa Institute, Nagoya University, Nagoya, Japan

- 106 ^(a) INFN Sezione di Napoli; ^(b) Dipartimento di Fisica, Università di Napoli, Napoli, Italy
- 107 Department of Physics and Astronomy, University of New Mexico, Albuquerque NM, United States
- 108 Institute for Mathematics, Astrophysics and Particle Physics, Radboud University Nijmegen/Nikhef, Nijmegen, Netherlands
- 109 Nikhef National Institute for Subatomic Physics and University of Amsterdam, Amsterdam, Netherlands
- 110 Department of Physics, Northern Illinois University, DeKalb IL, United States
- 111 Budker Institute of Nuclear Physics, SB RAS, Novosibirsk, Russia
- 112 Department of Physics, New York University, New York NY, United States
- 113 Ohio State University, Columbus OH, United States
- 114 Faculty of Science, Okayama University, Okayama, Japan
- 115 Homer L. Dodge Department of Physics and Astronomy, University of Oklahoma, Norman OK, United States
- 116 Department of Physics, Oklahoma State University, Stillwater OK, United States
- 117 Palacký University, RCPTM, Olomouc, Czech Republic
- 118 Center for High Energy Physics, University of Oregon, Eugene OR, United States
- 119 LAL, Univ. Paris-Sud, CNRS/IN2P3, Université Paris-Saclay, Orsay, France
- 120 Graduate School of Science, Osaka University, Osaka, Japan
- 121 Department of Physics, University of Oslo, Oslo, Norway
- 122 Department of Physics, Oxford University, Oxford, United Kingdom
- 123 ^(a) INFN Sezione di Pavia; ^(b) Dipartimento di Fisica, Università di Pavia, Pavia, Italy
- 124 Department of Physics, University of Pennsylvania, Philadelphia PA, United States
- 125 National Research Centre “Kurchatov Institute”, B.P. Konstantinov Petersburg Nuclear Physics Institute, St. Petersburg, Russia
- 126 ^(a) INFN Sezione di Pisa; ^(b) Dipartimento di Fisica E. Fermi, Università di Pisa, Pisa, Italy
- 127 Department of Physics and Astronomy, University of Pittsburgh, Pittsburgh PA, United States
- 128 ^(a) Laboratório de Instrumentação e Física Experimental de Partículas - LIP, Lisboa; ^(b) Faculdade de Ciências, Universidade de Lisboa, Lisboa; ^(c) Department of Physics, University of Coimbra, Coimbra; ^(d) Centro de Física Nuclear da Universidade de Lisboa, Lisboa; ^(e) Departamento de Física, Universidade do Minho, Braga; ^(f) Departamento de Física Teórica y del Cosmos and CAFPE, Universidad de Granada, Granada, Spain; ^(g) Dep. Física and CEFITEC of Faculdade de Ciências e Tecnologia, Universidade Nova de Lisboa, Caparica, Portugal
- 129 Institute of Physics, Academy of Sciences of the Czech Republic, Praha, Czech Republic
- 130 Czech Technical University in Prague, Praha, Czech Republic
- 131 Charles University, Faculty of Mathematics and Physics, Prague, Czech Republic
- 132 State Research Center Institute for High Energy Physics (Protvino), NRC KI, Russia
- 133 Particle Physics Department, Rutherford Appleton Laboratory, Didcot, United Kingdom
- 134 ^(a) INFN Sezione di Roma; ^(b) Dipartimento di Fisica, Sapienza Università di Roma, Roma, Italy
- 135 ^(a) INFN Sezione di Roma Tor Vergata; ^(b) Dipartimento di Fisica, Università di Roma Tor Vergata, Roma, Italy
- 136 ^(a) INFN Sezione di Roma Tre; ^(b) Dipartimento di Matematica e Fisica, Università Roma Tre, Roma, Italy
- 137 ^(a) Faculté des Sciences Ain Chock, Réseau Universitaire de Physique des Hautes Energies - Université Hassan II, Casablanca; ^(b) Centre National de l’Energie des Sciences Techniques Nucleaires, Rabat; ^(c) Faculté des Sciences Semlalia, Université Cadi Ayyad, LPHEA-Marrakech; ^(d) Faculté des Sciences, Université Mohamed Premier and LPTPM, Oujda; ^(e) Faculté des sciences, Université Mohammed V, Rabat, Morocco
- 138 DSM/IRFU (Institut de Recherches sur les Lois Fondamentales de l’Univers), CEA Saclay (Commissariat à l’Energie Atomique et aux Energies Alternatives), Gif-sur-Yvette, France
- 139 Santa Cruz Institute for Particle Physics, University of California Santa Cruz, Santa Cruz CA, United States
- 140 Department of Physics, University of Washington, Seattle WA, United States
- 141 Department of Physics and Astronomy, University of Sheffield, Sheffield, United Kingdom
- 142 Department of Physics, Shinshu University, Nagano, Japan
- 143 Department Physik, Universität Siegen, Siegen, Germany
- 144 Department of Physics, Simon Fraser University, Burnaby BC, Canada
- 145 SLAC National Accelerator Laboratory, Stanford CA, United States
- 146 ^(a) Faculty of Mathematics, Physics & Informatics, Comenius University, Bratislava; ^(b) Department of Subnuclear Physics, Institute of Experimental Physics of the Slovak Academy of Sciences, Kosice, Slovak Republic
- 147 ^(a) Department of Physics, University of Cape Town, Cape Town; ^(b) Department of Physics, University of Johannesburg, Johannesburg; ^(c) School of Physics, University of the Witwatersrand, Johannesburg, South Africa
- 148 ^(a) Department of Physics, Stockholm University; ^(b) The Oskar Klein Centre, Stockholm, Sweden
- 149 Physics Department, Royal Institute of Technology, Stockholm, Sweden
- 150 Departments of Physics & Astronomy and Chemistry, Stony Brook University, Stony Brook NY, United States
- 151 Department of Physics and Astronomy, University of Sussex, Brighton, United Kingdom
- 152 School of Physics, University of Sydney, Sydney, Australia
- 153 Institute of Physics, Academia Sinica, Taipei, Taiwan
- 154 Department of Physics, Technion: Israel Institute of Technology, Haifa, Israel
- 155 Raymond and Beverly Sackler School of Physics and Astronomy, Tel Aviv University, Tel Aviv, Israel
- 156 Department of Physics, Aristotle University of Thessaloniki, Thessaloniki, Greece
- 157 International Center for Elementary Particle Physics and Department of Physics, The University of Tokyo, Tokyo, Japan
- 158 Graduate School of Science and Technology, Tokyo Metropolitan University, Tokyo, Japan
- 159 Department of Physics, Tokyo Institute of Technology, Tokyo, Japan
- 160 Tomsk State University, Tomsk, Russia
- 161 Department of Physics, University of Toronto, Toronto ON, Canada
- 162 ^(a) INFN-TIFPA; ^(b) University of Trento, Trento, Italy
- 163 ^(a) TRIUMF, Vancouver BC; ^(b) Department of Physics and Astronomy, York University, Toronto ON, Canada
- 164 Faculty of Pure and Applied Sciences, and Center for Integrated Research in Fundamental Science and Engineering, University of Tsukuba, Tsukuba, Japan
- 165 Department of Physics and Astronomy, Tufts University, Medford MA, United States
- 166 Department of Physics and Astronomy, University of California Irvine, Irvine CA, United States
- 167 ^(a) INFN Gruppo Collegato di Udine, Sezione di Trieste, Udine; ^(b) ICTP, Trieste; ^(c) Dipartimento di Chimica, Fisica e Ambiente, Università di Udine, Udine, Italy
- 168 Department of Physics and Astronomy, University of Uppsala, Uppsala, Sweden
- 169 Department of Physics, University of Illinois, Urbana IL, United States
- 170 Instituto de Física Corpuscular (IFIC) and Departamento de Física Atomica, Molecular y Nuclear and Departamento de Ingeniería Electrónica and Instituto de Microelectrónica de Barcelona (IMB-CNM), University of Valencia and CSIC, Valencia, Spain
- 171 Department of Physics, University of British Columbia, Vancouver BC, Canada
- 172 Department of Physics and Astronomy, University of Victoria, Victoria BC, Canada
- 173 Department of Physics, University of Warwick, Coventry, United Kingdom
- 174 Waseda University, Tokyo, Japan
- 175 Department of Particle Physics, The Weizmann Institute of Science, Rehovot, Israel
- 176 Department of Physics, University of Wisconsin, Madison WI, United States
- 177 Fakultät für Physik und Astronomie, Julius-Maximilians-Universität, Würzburg, Germany

¹⁷⁸ Fakultät für Mathematik und Naturwissenschaften, Fachgruppe Physik, Bergische Universität Wuppertal, Wuppertal, Germany

¹⁷⁹ Department of Physics, Yale University, New Haven CT, United States

¹⁸⁰ Yerevan Physics Institute, Yerevan, Armenia

¹⁸¹ Centre de Calcul de l'Institut National de Physique Nucléaire et de Physique des Particules (IN2P3), Villeurbanne, France

^a Also at PKU-CHEP.

^b Also at Department of Physics, King's College London, London, United Kingdom.

^c Also at Institute of Physics, Azerbaijan Academy of Sciences, Baku, Azerbaijan.

^d Also at Novosibirsk State University, Novosibirsk, Russia.

^e Also at TRIUMF, Vancouver BC, Canada.

^f Also at Department of Physics & Astronomy, University of Louisville, Louisville, KY, United States of America.

^g Also at Physics Department, An-Najah National University, Nablus, Palestine.

^h Also at Department of Physics, California State University, Fresno CA, United States of America.

ⁱ Also at Department of Physics, University of Fribourg, Fribourg, Switzerland.

^j Also at II Physikalisches Institut, Georg-August-Universität, Göttingen, Germany.

^k Also at Departament de Física de la Universitat Autònoma de Barcelona, Barcelona, Spain.

^l Also at Departamento de Física e Astronomia, Faculdade de Ciências, Universidade do Porto, Portugal.

^m Also at Tomsk State University, Tomsk, Russia, Russia.

ⁿ Also at The Collaborative Innovation Center of Quantum Matter (CICQM), Beijing, China.

^o Also at Università di Napoli Parthenope, Napoli, Italy.

^p Also at Institute of Particle Physics (IPP), Canada.

^q Also at Horia Hulubei National Institute of Physics and Nuclear Engineering, Bucharest, Romania.

^r Also at Department of Physics, St. Petersburg State Polytechnical University, St. Petersburg, Russia.

^s Also at Borough of Manhattan Community College, City University of New York, New York City, United States of America.

^t Also at Department of Physics, The University of Michigan, Ann Arbor MI, United States of America.

^u Also at Centre for High Performance Computing, CSIR Campus, Rosebank, Cape Town, South Africa.

^v Also at Louisiana Tech University, Ruston LA, United States of America.

^w Also at Institutio Catalana de Recerca i Estudis Avancats, ICREA, Barcelona, Spain.

^x Also at Graduate School of Science, Osaka University, Osaka, Japan.

^y Also at Fakultät für Mathematik und Physik, Albert-Ludwigs-Universität, Freiburg, Germany.

^z Also at Institute for Mathematics, Astrophysics and Particle Physics, Radboud University Nijmegen/Nikhef, Nijmegen, Netherlands.

^{aa} Also at Department of Physics, The University of Texas at Austin, Austin TX, United States of America.

^{ab} Also at Institute of Theoretical Physics, Ilia State University, Tbilisi, Georgia.

^{ac} Also at CERN, Geneva, Switzerland.

^{ad} Also at Georgian Technical University (GTU), Tbilisi, Georgia.

^{ae} Also at Ochadai Academic Production, Ochanomizu University, Tokyo, Japan.

^{af} Also at Manhattan College, New York NY, United States of America.

^{ag} Also at Academia Sinica Grid Computing, Institute of Physics, Academia Sinica, Taipei, Taiwan.

^{ah} Also at School of Physics, Shandong University, Shandong, China.

^{ai} Also at Departamento de Física Teórica y del Cosmos and CAFPE, Universidad de Granada, Granada (Spain), Portugal.

^{aj} Also at Department of Physics, California State University, Sacramento CA, United States of America.

^{ak} Also at Moscow Institute of Physics and Technology State University, Dolgoprudny, Russia.

^{al} Also at Departement de Physique Nucleaire et Corpusculaire, Université de Genève, Geneva, Switzerland.

^{am} Also at International School for Advanced Studies (SISSA), Trieste, Italy.

^{an} Also at Institut de Física d'Altes Energies (IFAE), The Barcelona Institute of Science and Technology, Barcelona, Spain.

^{ao} Also at School of Physics, Sun Yat-sen University, Guangzhou, China.

^{ap} Also at Institute for Nuclear Research and Nuclear Energy (INRNE) of the Bulgarian Academy of Sciences, Sofia, Bulgaria.

^{aq} Also at Faculty of Physics, M.V. Lomonosov Moscow State University, Moscow, Russia.

^{ar} Also at Institute of Physics, Academia Sinica, Taipei, Taiwan.

^{as} Also at National Research Nuclear University MEPhI, Moscow, Russia.

^{at} Also at Department of Physics, Stanford University, Stanford CA, United States of America.

^{au} Also at Institute for Particle and Nuclear Physics, Wigner Research Centre for Physics, Budapest, Hungary.

^{av} Also at Giresun University, Faculty of Engineering, Turkey.

^{aw} Also at CPPM, Aix-Marseille Université and CNRS/IN2P3, Marseille, France.

^{ax} Also at Department of Physics, Nanjing University, Jiangsu, China.

^{ay} Also at University of Malaya, Department of Physics, Kuala Lumpur, Malaysia.

^{az} Also at LAL, Univ. Paris-Sud, CNRS/IN2P3, Université Paris-Saclay, Orsay, France.

* Deceased.